Deep genetic divergence and cytonuclear discordance in the grasshopper *Oedaleus decorus*

Masterarbeit

der Philosophisch-naturwissenschaftlichen Fakultät

der Universität Bern

vorgelegt von

Eveline Kindler

2010

Leiter der Arbeit:

PD. Dr. Gerald Heckel

Computational and Molecular Population Genetics

Prof. Dr. Raphaël Arlettaz

Conservation Biology

Institute of Ecology and Evolution

Table of contents

Abstract

The grasshopper *Oedaleus decorus* is a thermophilic insect with a prevalent southern distribution range, stretching from the Mediterranean regions as far as to Central-Asia and China and it can be found in the steppes of almost entire Africa. Given this broad range and the world-importance as a pest-species to agriculture, it is surprising no range-wide study has been conducted so far. In this study we included up to 254 fresh samples and dry museum specimens of *O. decorus* to cover 25 localities across Europe. Maternally inherited mitochondrial markers (mtDNA) revealed a surprisingly deep genetic split in this species into an Eastern and a Western lineage, potentially pre-dating the last glacial maximum. However, only the combination with eleven biparentally inherited microsatellite loci (nucDNA) had the potential to uncover a contrasting pattern between mtDNA and nucDNA in the well known Alpine suture-zone. We found evidence of cytonuclear discordance in one population in northern Italy, in which all individuals are exclusively part of the Eastern mtDNA lineage. However, according to Bayesian assignment methods based on microsatellite loci, the individuals clustered with genotypes from the Western mtDNA lineage. We suggest that this lack of congruence between the two markers could be due to strong male-biased dispersal which led to gene flow between the two divergent lineages, but meanwhile conserved the phylogeographic mtDNA pattern. As an alternative, introgression from individuals of the Eastern mtDNA lineage into the gene pool of the invading individuals from the Western mtDNA lineage is quite compatible with our results as well. Our study explicitly indicates the importance of multilocus frameworks, as the interpretation of mtDNA data alone would have led to the biased conclusions of two highly divergent lineages with no admixture and microsatellite data only, would have revealed too little differentiation.

Introduction

The last glacial period in the Pleistocene had dramatic consequences on the survival and distribution of various taxa present today (Hewitt, 1996). The huge ice cover and the reduction of temperature led to the extinction of some cold-intolerant species and to latitudinal and altitudinal shifts into more favourable habitats (Hewitt, 1999; Hewitt, 2004). Iberia, the Italian peninsula and the Balkans are widely accepted as the three major southern refugia for several European temperate species (Hewitt, 1999; Hewitt, 2004; Taberlet *et al.*, 1998). The refugial areas in the South were mainly characterized by semi-desert steppes and grassy vegetation with patches of trees in moist areas (Ray & Adams, 2001). Additional northern or south-eastern retreat areas were suggested for organisms able to tolerate cold conditions such as the common vole (Microtus arvalis; Fink *et al.*, 2004; Heckel *et al.*, 2005), the bank vole (Clethrionomys glareolus; Kotlik *et al.*, 2006) and the European ground squirrel (Spermophilus citellus; Krystufek *et al.*, 2009). Long-term isolation of populations in refugia may promote allopatric divergence and accordingly the formation of distinct genetic lineages (Hewitt, 2000). Expansions from refugial areas during the inter-glacials may have led to secondary contact between previously isolated genomes and potentially to the re-establishment of gene flow (Canestrelli *et al.*, 2006) or to partial introgression (Alves *et al.*, 2008). In Europe, one of the most obvious suture-zone is the Alpine barrier which separates lineages in Italy from lineages in the west and in the north of the mountains (Taberlet *et al.*, 1998). However, the impact of the last glacial maximum (LGM) on thermophilic species inhabiting steppe-like habitats has received less attention so far. Herterich (1991) and Schmitt *et al*. (2003) suggested that two climatically favourable areas in the southwest and southeast of the Iberian Peninsula acted as refugia for xero-thermophilic organisms such as the butterfly *Aglaope infausta*. Schmitt (2007) further proposed the more southern and warmer Maghreb in Northern Africa as the centre of origin for some thermophilic species rather than Iberia.

In this study we investigated the evolutionary history of an obligatory thermophilic grasshopper species with a prevalent southern distribution range. The study species is the acridid grasshopper *Oedaleus decorus* (Orthoptera, Germar 1826) which is a xero-thermophilic and stenothermic insect inhabiting steppe-like areas at sunny sites with a high amount of bare ground (Bellmann, 2006; Ingrisch & Köhler, 1998; Monnerat *et al.*, 2007; Schmidt & Lilge, 1996; Tami & Fontana, 2002). The low tolerance for other habitat types makes it extremely sensitive to environmental changes. Harz (1975), Schmidt & Lilge (1996), Boczki (2007) and Yin *et al.* (2008) suggested long distance flights and large population sizes as characteristics for this macropterous grasshopper which have probably been helpful features in maintaining its broad distribution range. Although the Palearctic and Afrotropical distribution of *O. decorus* (Baur *et al.*, 2006; Fet, 2007) and its world-importance as a pest for agriculture (Yin *et al.*, 2008), no range-wide study about this species has been conducted so far. Fries *et al*. (2007) inferred the taxonomic status of *O. decorus* and *O. asiaticus* based on four mitochondrial genes (*COI*, *COII*, *cytb*, *ND5*) and molecular data of other Oedipodinae. The authors concluded that *O. asiaticus* is the sister species of *O. decorus* and further estimated a split between them 35Ma (million years ago). Previous work has shown that the taxonomic status of the two former subspecies *Oedaleus decorus decorus* and *Oedaleus decorus asiaticus* (Bei-Bienko, 1941; Ma *et al.*, 2009) as full species is still under debate. The latter taxon replaces *O. decorus* in the Mongolian Plateau and in the Transbaikal region of southern Russia (Ritchie, 1981).

The aim of this study was to investigate the evolutionary history and phylogenetic relationships of a thermophilic grasshopper species (*Oedaleus decorus*) with a predominant southern distribution in Europe. We further analysed the population structure in the Alpine region, which is well known for its importance as a suture-zone in various species. Further, genetic diversity was compared between populations inhabiting previously glaciated areas and populations from localities which were not affected by the ice-cover during the last glacial maximum. We used maternally inherited mtDNA markers to identify major evolutionary lineages in *O. decorus* across its distribution range in Europe and biparentally

inherited microsatellites (nucDNA) to resolve fine-scale structures in genetic variability in and around the Alps. However, there are some technical issues in the use of both markers which should be taken into account. The relatively high frequency of pseudogenes in some acridid grasshoppers may lead to incorrect phylogenetic inferences if they remain unrecognised (Arctander, 1995; Bensasson *et al.*, 2001; Bensasson *et al.*, 2000; Blanchard & Lynch, 2000; Song *et al.*, 2008; Zhang & Hewitt, 1996a; Zhang & Hewitt, 1996b). The potential presence of null alleles, the challenge of large genomes and longer alleles, on the other hand, are some possible issues of microsatellite analyses in certain Acrididae (Chapuis & Estoup, 2007; Ustinova *et al.*, 2006). But, several recent studies have illustrated the value of combining mtDNA and nucDNA markers to trace back the species history, to enlarge the temporal coverage of the study because both markers are informative over different time scales and to uncover discrepancies between both markers (Cicconardi *et al.*, 2009; Feulner *et al.*, 2004; Renoult *et al.*, 2009; Yang & Kenagy, 2009).

Materials and methods

The study species

Oedaleus decorus has a broad Palearctic distribution range (Baur *et al.*, 2006), stretching from the Mediterranean area as far as to Central-Asia and Kaltenbach (1970) and Fet (2007) suggested that the species is also widespread in the steppes of almost entire Africa up to the Afrotropical Region. In Southern Europe, the species has not been observed in Portugal yet (Ch. Bastos-Silveira, Natural History Museum, Lisbon), but in Central Europe, its presence is rather scattered and restricted. *O. decorus* is endangered in Slovenia (Gomboc & Trontelj, 2001) and rapidly declining in Switzerland where it is constricted to two isolated sites in the South (Monnerat *et al.*, 2007). The species is rarely found in Slovakia (Kočárek *et al.*, 1999) and became extinct in the 1940/50s in Austria (Berg & Zuna-Kratky, 1997) and in the Czech Republic (Holuša & Kočárek, 2005) where it reached its northern distribution limit (Kaltenbach, 1970). In France, the species is absent north of the river Seine (Bellmann & Luquet, 2009; Defaut *et al.*, 2009). Its presence in Germany was confirmed 50km north from the expansion limit in France (2007), but it is not certain if the species have flown in by it-self as a consequence of a summer heat-wave and beneficial south-west air currents or if it was introduced by humans.

Samples and DNA extraction

426 *Oedaleus decorus* and 71 *O. asiaticus* samples from 108 different localities across their distribution ranges in Europe, North-Africa and Central-Asia have been collected for this study (Appendixes 1 & 2). We analysed 276 *O. decorus* samples and three *O. asiaticus* specimen from 26 different localities with sample sizes varying between one and 37 individuals (Fig. 1, Table 1). Additional dry museum material from 150 *O. decorus* and 68 *O. asiaticus* could not be included in the dataset as either DNA extraction or subsequent amplification failed, even with internal primers and adjusted PCR protocols. An already

published sequence of *O. asiaticus* was included in the data set (GenBank, Accession no NC_011115; Ma *et al.*, 2009) and the closely related species *Gastrimargus marmoratus* (Acrididae, GenBank Accession no EU13373; Ma *et al.*, 2009) was used as outgroup to root the phylogenetic trees.

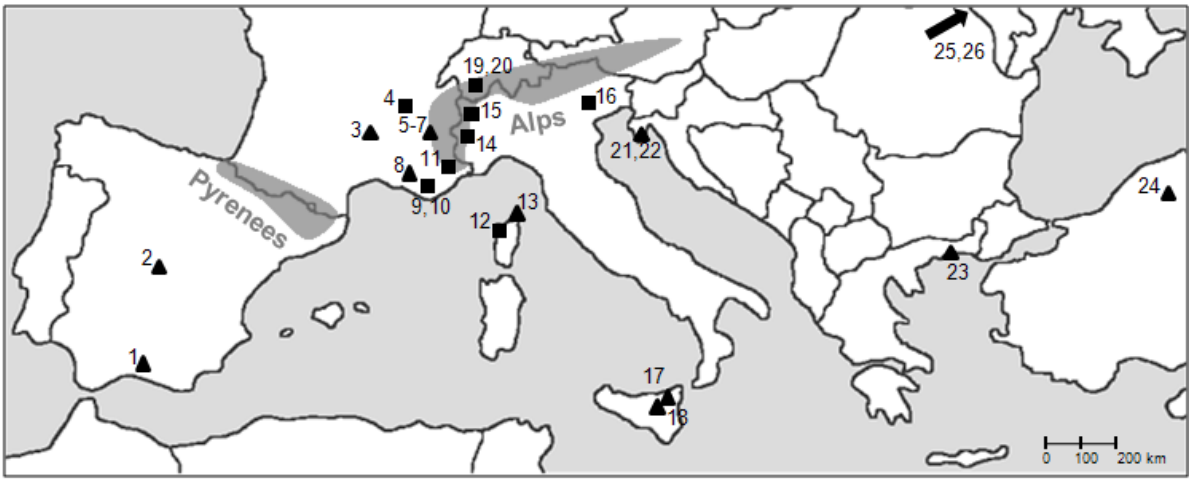

Fig. 1 Sampling sites of *Oedaleus decorus* across its distribution range in Europe. Triangles indicate sampling positions used for phylogeographic analyses only. Squares represent sampling locations additionally used for population genetic studies. Numbers and sample sizes are displayed in Table 1. The Alps and the Pyrenees are highlighted in grey. The arrow points toward the direction of the sampling locality in Russia and the sampling site of *Oedaleus asiaticus* in China.

Fresh *O. decorus* samples were collected between 2005 and 2009, stored in absolute ethanol at 4 °C, and genomic DNA was extracted exclusively from muscle tissue from hind legs following a standard phenol-chloroform protocol (Sambrook *et al.*, 1989). Genomic DNA from seven dry *O. decorus* and two dry *O. asiaticus* specimen was extracted according to an adapted phenol-chloroform protocol: first, hind legs were ground and the resulting homogeneous powder was digested with 30 µL proteinase K (10mg/ml) at 37 °C overnight. The following morning, 20 µL proteinase K was added and digestion was continued at 55 °C for 2 h. To achieve optimal precipitation, the samples were stored in pure ethanol at -20 °C overnight.

DNA sequencing

A 546 base-pair (bp) DNA fragment covering part of the mitochondrial 12S rRNA (120bp) and of the highly variable control region (ctr, 426bp) was amplified and sequenced from 170 ethanol preserved and five dry specimen. The newly developed primers Odec-dloop-F1 (5'-TGGCACGAAATATGCCAATA-3') and Odec-dloop-R3 (5'-CATTTAACTGAAT-GTAAGACCCATAC-3'; Appendix 3) were used for amplification in a reaction volume of 25 µL in a GeneAmp PCR System 9700 (Applied Biosystems; Appendix 4). The Polymerase Chain Reaction (PCR) conditions using QIAGEN *Taq* polymerase were the following: initial denaturation at 95 °C for 2 min, subsequent 35 cycles of denaturation at 94 °C for 30 s, annealing at 55 °C for 1 min, extension at 72 °C for 1 min and a final extension step at 72 °C for 10 min (Appendix 5). The PCR products were checked for successful amplification and correct size on a 1.5% agarose gel by comparing them to a 100bp ladder (Invitrogen). PCR products showing any sign of double bands were not further processed. The remaining products were cleaned using a GenElute PCR Clean-up kit (Sigma) following the manufacturer's protocol. Sequencing reactions using the forward primer Odec-dloop-F1 were carried out with the Terminator Ready Reaction Mix "Big Dye" (v 3.1, Applied Biosystems) in a reaction volume of 10 µL (Appendix 4). The reaction conditions were as follows: initial denaturation at 96 °C for 50 s, 35 cycles with denaturation at 96 °C for 10 s, annealing at 50 °C for 10 s and extension at 60 °C for 4 min 30 s (Appendix 5). The PCR products were purified according to a sodium-acetate precipitation protocol and then separated and detected on an ABI PRISM 3100 Genetic Analyzer (Applied Biosystems).

We used internal primers and a nested PCR to amplify mtDNA from five dry museum specimen as the amplification from museum material with the standard primers failed because of DNA fragmentation and low concentration. The resulting concatenated sequence was a shorter portion (376bp) of the original fragment (546bp). The amplification of a 5' fragment was carried out using Odec-dloop-F1 and the newly designed internal reverse primer Odec-dloop-int-R (5'-GGTTTGCGGGATATGTGTTC-3'), and for the amplification of a

downstream segment using the forward internal primer Odec-dloop-int-F (5'-GAACACATATCCCGCAAACC-3') and Odec-dloop-R3 (Appendixes 3 & 4). A nested PCR was used to increase the amount of the target sequence: initial denaturation at 95 °C for 2 min, followed by 40 cycles of denaturation at 94 °C for 30 s, annealing at 52 °C for 1 min, extension at 72 °C for 1 min and a final extension step at 72 °C for 10 min. In the successive amplification run, we used 1 µL of the amplified PCR products as template and the reaction conditions mentioned above. Direct sequencing was carried out for each of the four primers and the reaction was adjusted by increasing the amount of template DNA from 1 µL to 4 µL (Appendixes 4 & 5).

Table 1 Sampling sites of *Oedaleus decorus* and *Oedaleus asiaticus* with reference numbers from Figure 1. Given are sampling sites (label, country, location, latitude and longitude) and the number of samples analysed for mtDNA and nucDNA (*n*), respectively. Population samples are indicated in bold. * refers to dry museum material, () indicates dry museum specimen not included in the 546bp mtDNA alignment, ** specifies *Oedaleus asiaticus*.

Map ref.	Label	Country	Location	Latitude	Longitude	*n mtDNA*	*n nucDNA*
1	ECa	Spain	Capileira	36°57'N	03°21'W	5	
(2*)	EBe	Spain	Brunete	40°24'N	03°59'E	1	
3*	FMa	France	Saint-Ilpize à Saint-Marcel	45°11'N	03°23'E	1	
4	FVa	France	Valbonne	45°52'N	05°07'E	15	19
5	FRo	France	La Roche-de-Rame	44°45'N	06°34'E	1	
6	FAr	France	L'Argentière-la-Bessée	44°47'N	06°33'E	5	
7	FSt	France	Saint-Martin de Queyrières	44°50'N	06°35'E	5	
8*	FVe	France	Vergières	43°34'N	04°49'E	1	
9	FCr	France	Crau	43°08'N	06°04'E	15	20
10	FStMa	France	Saint-Martin de Crau	43°34'N	04°50'E	6	34
11	FSi	France	Sisteron	44°11'N	05°56'E	14	19
12	FPi	France, Corsica	Piana	42°14'N	08°38'E	13	24
13*	FFl	France, Corsica	Saint-Florent	42°40'N	09°18'E	1	
14	ISu	Italy	Susa	45°08'N	07°02'E	14	27
15	ICo	Italy	Cogne	45°36'N	07°22'E	14	20
16	IMa	Italy	Magredi	46°04'N	12°44'E	17	37
(17*)	IRN	Italy	Rocca di Novara	38°02'N	15°05'E	1	
(18*)	IRa	Italy	Randazzo	37°52'N	14°57'E	1	
19	CHOs	Switzerland	Ossona	46°10'N	07°25'E	20	21
20	CHGa	Switzerland	Gampel	46°18'N	07°44'E	17	20
21	HRVo	Croatia	Voz	45°13'N	14°34'E	5	
22	HROb	Croatia	Obzovo	44°58'N	14°45'E	3	
(23*)	GRNk	Greece	Nea Karvali	40°57'N	24°30'E	1	
(24)	TCa	Turkey	Çankırı	40°50'N	32°45'E	1	
25	RKur	Russia	Kurgan	54°37'N	64°27'E	1	
26**	CNXi	China	Xilinhot	43°57'N	116°08'E	3	

Pseudogenes and phylogenetic inferences

In order to minimize the potential presence of pseudogenes, DNA was exclusively extracted from muscle tissue rich in mitochondria to enhance the relative amount of mitochondrial DNA compared to nuclear DNA. Amplified PCR products were carefully checked for double-bands and samples showing ambiguous sequences were not included in further analyses. Dry museum samples were amplified with two different primer pairs, thus, a possible nuclear origin of their sequence was minimized. As Ma *et al*. (2009) used isolated mitochondria for sequencing the complete mitochondrial genome of *Oedaleus asiaticus* and as the two *O. asiaticus* samples in our study showed the same haplotype, we can verify their mitochondrial origin. Several samples were additionally amplified and sequenced for the mitochondrial gene *ND2*. Translation of the sequences did not reveal any premature stop codons which might have been an indication of nuclear copies. Phylogenetic relationships in either case were simultaneously inferred with Bayesian and neighbour-joining algorithms.

Microsatellite genotyping

Nuclear DNA of 241 samples from ten populations (Table 1) was analysed at the following 11 microsatellite loci in two separate multiplex sets: *OD2*, *OD4*, *OD6*, *OD7*, *OD9*, *OD12* and *OD3*, *OD5*, *OD8*, *OD18*, *OD31* (Berthier *et al.*, 2008; Appendix 6). PCR amplifications with fluorescently labelled forward and unlabeled reverse primers were performed with the QIAGEN Multiplex Kit using thermal cyclers GeneAmp PCR System 9700 (Applied Biosystems) in a 10 µL reaction volume and the following conditions (Appendixes 4-7): Taq activation at 96 °C for 15 min, followed by 30 cycles of denaturation at 94 °C for 30 s, annealing at 57 °C for 1 min and 30 s, extension at 72 °C for 60 s and final extension at 60 °C for 30 min. Fragments were separated by electrophoresis on an ABI 3100 Sequencer (Applied Biosystems) and their length was determined using GeneMapper software v.3.7 (Applied Biosystems) against an internal size standard (GeneScan TM-500LIZ™ Applied

Biosystems). Loci which failed to amplify were repeated following an adjusted amplification protocol:initial denaturation at 94 °C for 5 min, subsequent 30 cycles of denaturation at 94 °C for 1 min, annealing at 53 °C for 1 min, extension at 72 °C for 1 min and 15 s and a final extension step at 72 °C for 10 min (Appendixes 4 & 5). Repetitions of previously analysed individuals were used to ensure consistency of genotyping (Schweizer *et al.*, 2007).

Phylogenetic analyses of mtDNA

Sequences of mtDNA were aligned using the CLUSTALW algorithm (Thompson *et al.*, 1997) implemented in BIOEDIT v.7.0 (Hall, 1999) and revised manually. The number of segregating sites as well as the identity and frequency of haplotypes was determined using ARLEQUIN v.3.5 (Excoffier & Lischer, in prep). Redundant haplotypes were removed from phylogenetic analyses. Phylogenetic relationships were determined by neighbour-joining algorithms (NJ; Saitou & Nei, 1987) implemented in MEGA v.3.1 (Kumar *et al.*, 2004) and by Bayesian algorithms implemented in MRBAYES v.3.1.2 (Huelsenbeck & Ronquist, 2001; Ronquist & Huelsenbeck, 2003). The general time-reversible model (GTR; Tavaré, 1986; Tavaré *et al.*, 1997) with a proportion of invariable sites (I; Gu *et al.*, 1995) and a gamma-shaped distribution of rates across sites (Γ; Felsenstein, 2004) was selected as the optimal mutation model based on the Akaike Information Criterion (AIC; Akaike, 1974) implemented in JMODELTEST v.0.1.1 (Posada, 2008). The Bayesian analyses were run for 1 million generations with every 10^{th} generation sampled, using one cold and three heated chains. The first 25'000 (25%) samples were discarded as burn-in and convergence was determined by examining the log likelihood values, the split frequencies and by using TRACER v.1.4 (Rambaut & Drummod, 2007). The trees were visualized in TREEVIEW (Page, 1996). Phylogenetic relationships were inferred first for the shorter alignment with all samples mentioned in Table 1 and second for the longer fragment for which the five museum specimen indicated in the same table could not be included. The level of genetic differentiation between and within major evolutionary lineages was assessed with an

Analysis of Molecular Variance implemented in ARLEQUIN (AMOVA; Excoffier *et al.*, 1992). Tamura & Nei's substitution model (Tamura & Nei, 1993) was used and statistical significance was tested by 10.000 permutations. Net average divergence and pairwise difference among lineages was computed with MEGA based on 546bp mtDNA and using the Kimura-2-parameter model (Kimura, 1980).

Statistical analyses of population samples

Mitochondrial DNA. The number of haplotypes (*A*), haplotype (*h*) and nucleotide (π) diversity and the average number of nucleotide differences (k_1) was estimated for 145 samples (546bp mtDNA) from ten different populations using ARLEQUIN and DNASP v.5.0 (Librado & Rozas, 2009). Haplotype diversity within populations located at previously glaciated sites was compared to the variability in populations outside the glaciers range. Statistical significance was tested with a Kruskal-Wallis rank sum test in R v.2.10.0 (R Development Core Team, 2009). ARLEQUIN was used to perform a hierarchical AMOVA and to calculate overall and pairwise Φ_{ST} - values. Statistical significance was tested by 10.000 permutations and significance levels were corrected using the Bonferroni-Holm procedure (Holm, 1979). To check for an isolation-by-distance pattern (IBD; Rousset, 1997) we assessed the correlation between matrices of geographical distances expressed in log kilometres and pairwise linearized Φ_{ST} - values. The significance of the correlation was measured by Mantel tests using 999 permutations in GENALEX v.6.2 (Peakall & Smouse, 2006).

Microsatellites. The number of alleles, heterozygosity per locus and deviation from Hardy-Weinberg equilibrium (HWE) were computed using GENALEX and ARLEQUIN. Null allele frequencies at each locus for each population were estimated based on Expectation Maximization (EM) algorithms implemented in FREENA (Chapuis & Estoup, 2007). Allelic richness (k_2), observed (H_O) and expected heterozygosity (H_E) were calculated for each population with FSTAT v.2.9.3.2 (Goudet, 2001) and ARLEQUIN. Allelic richness within

populations located at previously glaciated sites was compared to the variability in populations located outside the glaciers range. Statistical significance was tested with a Kruskal-Wallis rank sum test in R. As for the mtDNA data set we performed an AMOVA to estimate overall F_{ST}. Pairwise F_{ST} values among populations were calculated to compare them to Φ_{ST} - values based on mtDNA data. In addition, F_{ST} corrected for the presence of null alleles were computed ($F_{ST}^{(ENA)}$) with the program FREENA. Linearized genetic distances F_{ST} / (1 - F_{ST}) were correlated against log-transformed geographic distances to test for an isolation-by-distance pattern using Mantel tests with 999 permutations in GENALEX. Principal Coordinate Analyses (PCoA) based on individual genotype data were performed with the same program to visualize genetic differentiation. Furthermore, we used STRUCTURE v.2.3 (Pritchard *et al.*, 2000) to assign individuals to different clusters. This Bayesian approach is based on genotype information only, which estimates the number of genetic clusters (*K*) in a data set, and assigns the individuals to them thereafter. We assumed an admixture model with correlated allele frequencies (Falush *et al.*, 2003), 500.000 Markov chain Monte Carlo (MCMC) iterations and a burn-in of 100.000 iterations. We ran 10 independent runs for *K* = 1 to 10 to detect potential “cryptic” population structure. The method suggested by Evanno *et al*. (2005) was used to estimate the most likely number of clusters. Figures were displayed using DISTRUCT v.1.1 (Rosenberg, 2004).

Results

Phylogenetic relationships

Within the 376bp sequences of 178 *O. decorus* a total of 38 variable sites were detected (Appendix 8A). These variable sites described the 18 distinct haplotypes displayed in Fig. 2. The most common haplotype H04 was found in 14 out of 25 locations covering Spain, France, Italy and Switzerland (Appendix 9A). Analysis of the 546 aligned nucleotide positions of 173 *O. decorus* individuals revealed 50 variable sites, which defined the 18 haplotypes shown in Fig. 3 (Appendix 8B). The most widespread haplotype H04 was found in 11 out of 20 locations in Spain, France, Italy and Switzerland. Haplotype sharing occurred most often between geographically close sites (e.g., Ossona, Gampel and Valbonne, Saint-Ilpize à Saint-Marcel or between Voz and Obzovo). Shared haplotypes were additionally found among Sisteron (Southern France) and Corsica (Appendix 9B).

Phylogenetic analyses revealed two evolutionary lineages in *O. decorus* in Europe well supported by Bayesian and neighbour-joining algorithms (Fig. 2 & 3). Haplotypes found in the eastern part of the European distribution range of *O. decorus* formed a highly divergent lineage relative to the other *O. decorus* lineage and to *O. asiaticus.* Genetic divergence among the two main lineages in *O. decorus* ranged from 6.8 to 7.7% (Table 2). Divergence to *O. asiaticus* was much higher for the Eastern lineage (7.9-8.4 %) than for the Western lineage (4.7-5.5 %). *G. marmoratus* differed by about 21% from both lineages found in *O. decorus* and from the sequence of *O. asiaticus.* Phylogenetic inferences based on *ND2* supported the mtDNA split in *O. decorus* into an Eastern and a Western lineage, but the relationship of the two lineages to *O. asiaticus* could not be fully resolved (Appendix 15). The Eastern lineage includes specimens from Russia, Turkey, Greece and Croatia, but individuals from the population from Northern Italy (Cogne) were part of this Eastern lineage as well. Two haplotypes from Southern Italy were basal to the second lineage (Fig. 2), which comprises samples from Spain, France, Italy and Switzerland. Within this Western lineage, haplotype

(H08, H09) from Switzerland (Ossona, Gampel) and from two northern locations in France (Valbonne, Saint-Ilpize à Saint-Marcel) formed a separate cluster based on Bayesian algorithms, but neighbour-joining algorithms did not support this substructure (Fig. 3). Haplotypes from Corsica and some individuals from Sisteron in Southern France (H11, H12) clustered together (Fig. 3), supported by Bayesian and neighbour-joining algorithms.

Table 2 Divergence among the Eastern (Russia, Croatia, Italy) and Western lineage (Spain, France, Italy, Switzerland) of *Oedaleus decorus*, *Oedaleus asiaticus* and the outgroup *Gastrimargus marmoratus* based on the Kimura-2-parameter model. Net average pairwise divergence is given above and pairwise divergence below the diagonal. All values are in percent. The highest divergence apart from the outgroup *G. marmoratus* was found between the Eastern lineage and *O. asiaticus*.

	Eastern lineage	Western lineage	*O. asiaticus*	*G. marmoratus*
Eastern lineage	-	6.9	7.9	20.7
Western lineage	6.8 - 7.7	-	4.8	20.4
O. asiaticus	7.9 - 8.4	4.7 - 5.5	-	21.2
G. marmoratus	20.7 - 21.0	20.4 - 21.0	21.2	-

Genetic variability in populations

Polymorphism in mtDNA covered a wide range with no variability in the populations from Gampel, Saint-Martin de Crau, Valbonne, Cogne, and Magredi up to a haplotype diversity (h) of 0.76 in Sisteron. Nucleotide diversity (π) ranged from zero to 0.46 (Sisteron) and average number of nucleotide differences (k_1) from zero to 2.54 (Sisteron), respectively. Haplotype diversity in populations inhabiting previously glaciated areas ranged from zero (Gampel, Cogne) to 0.28 in Ossona, and from zero (Saint-Martin de Crau, Valbonne, Magredi) to 0.76 (Sisteron) in populations from locations not affected by the ice-cover during the LGM (Table 3). Haplotype diversity was not significantly different between populations from previously glaciated areas compared to populations from localities not affected by the ice-cover (X^2 = 0.173; P = 0.68). Genetic variability at the microsatellite loci ranged from 25 to 59 alleles with

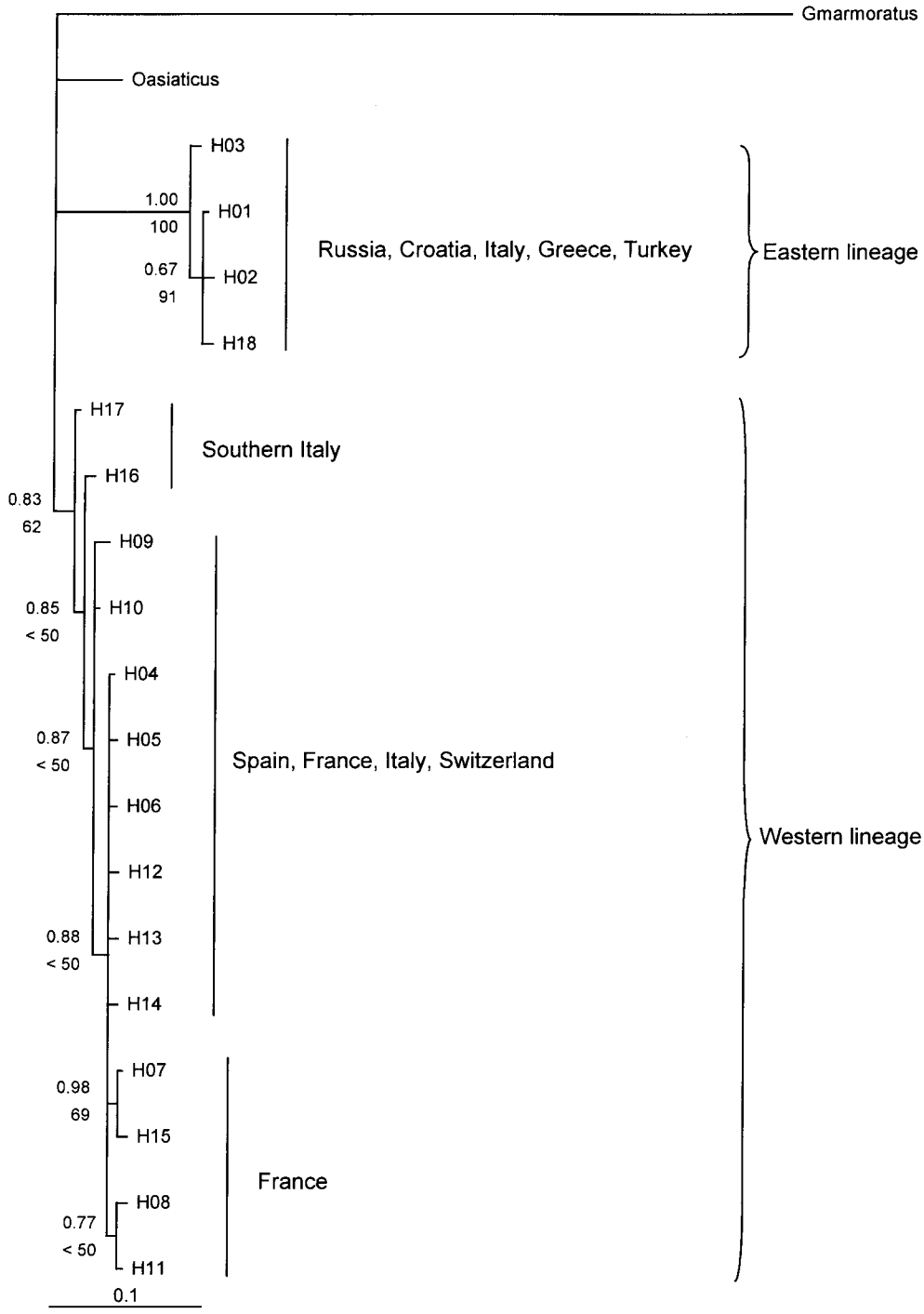

Fig. 2 Bayesian reconstruction of phylogenetic relationships based on 376bp mtDNA (12S rRNA; ctr) haplotypes from *Oedaleus decorus* and *Oedaleus asiaticus* with *Gastrimargus marmoratus* as outgroup. Posterior probabilities are indicated above the branches and percentage of bootstrap support for neighbour-joining algorithms below the branches. Haplotypes are listed in Appendix 9A.

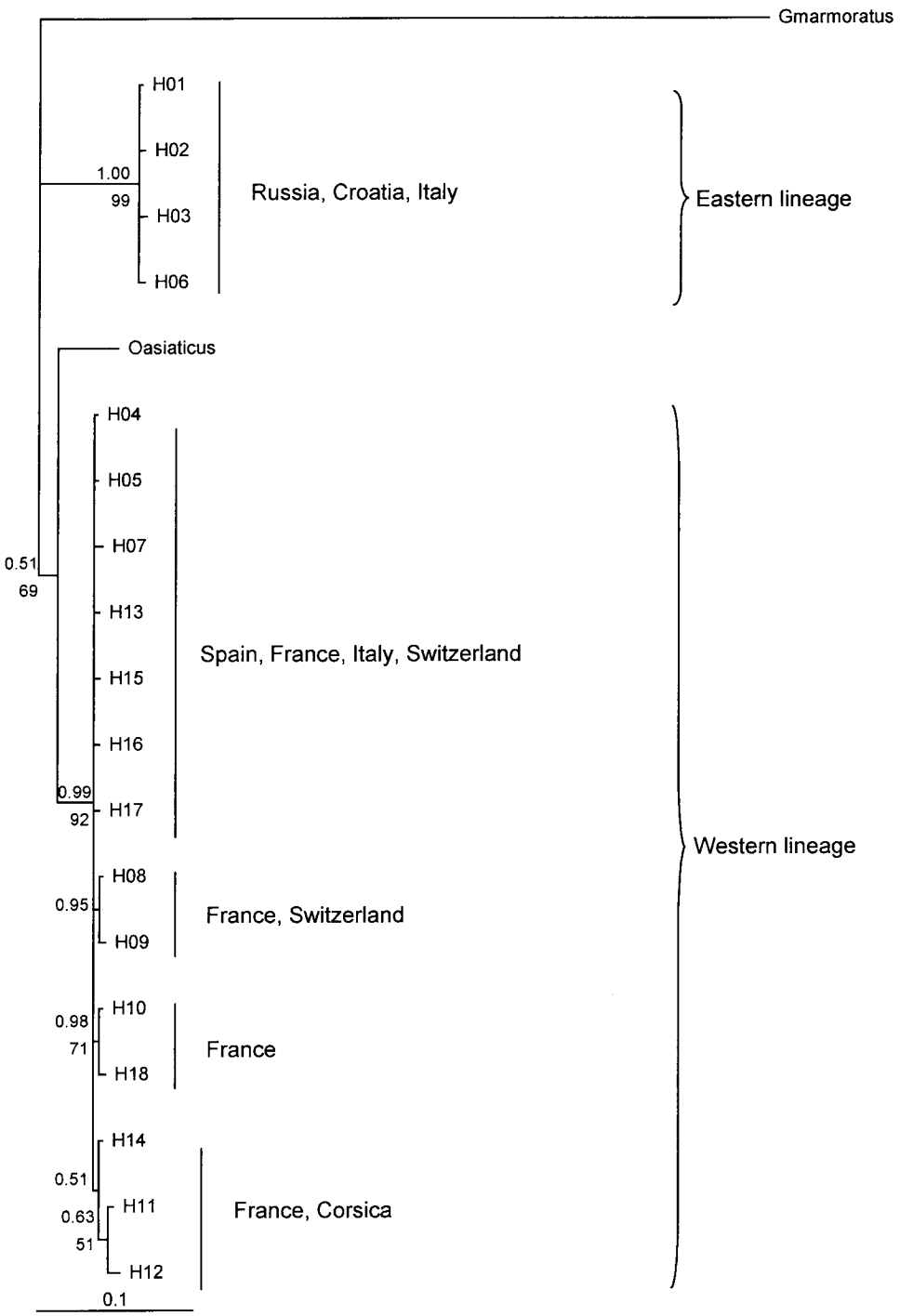

Fig. 3 Bayesian reconstruction of phylogenetic relationships based on 546bp mtDNA (12S rRNA; ctr) haplotypes from *Oedaleus decorus* and *Oedaleus asiaticus* with *Gastrimargus marmoratus* as outgroup. Posterior probabilities are indicated above the branches and percentage of bootstrap support for neighbour-joining algorithms below the branches. Branches with no bootstrap support were not resolved by neighbour-joining algorithms. Haplotypes are listed in Table 3 and Appendix 9B.

a mean of 43.92 overall (Appendix 10). Mean observed heterozygosity ranged from 0.61 (Cogne) to 0.78 (Sisteron) and mean allelic richness (k_2) per population ranged from 7.53 (Susa) to 16.81 (Saint-Martin de Crau). Allelic richness ranged from 7.53 (Susa) to 10.61 (Ossona) in populations from previously glaciated areas and from 13.90 (Valbonne) to 16.81 (Saint-Martin de Crau) in populations from locations not under ice-cover during the LGM, respectively (Table 3). Populations from localities affected by the glacier during the last ice-age showed significantly lower allelic richness than populations outside the glaciated area ($X^2 = 14.79$; $P < 0.001$).

Table 3 Genetic variation of ten *Oedaleus decorus* populations analysed for mtDNA and 11 microsatellite loci. For each locality the situation during the Last Glacial Maximum (LGM) (Ch. Schlüchter, Institute of Geological Sciences, Berne) the number of individuals analysed for mtDNA (n_1) and nucDNA (n_2) and the haplotype identification (H) is given. The following parameters were estimated: number of haplotypes (A), haplotype diversity (h), nucleotide diversity (π), average number of nucleotide differences (k_1), mean allelic richness (k_2), mean observed (H_O) and mean expected (H_E) heterozygosity.

			mtDNA						nucDNA			
Map ref.	Label	Glaciated	n_1	H	A	$h \pm SD$	π (%) $\pm SD$	k_1	n_2	k_2	H_O	H_E
19	CHOs	yes	20	H04, H08, H09	3	0.28 ± 0.12	0.05 ± 0.02	0.29	21	10.61	0.62	0.84
20	CHGa	yes	17	H08	1	0	0	0	20	8.32	0.67	0.82
9	FCr	no	15	H04, H10, H16 - H18	5	0.48 ± 0.16	0.12 ± 0.05	0.65	20	16.09	0.67	0.95
12	FPi	no	13	H11, H12	2	0.28 ± 0.15	0.22 ± 0.02	1.22	24	14.97	0.77	0.92
11	FSi	no	14	H04, H10 - H15	7	0.76 ± 0.10	0.46 ± 0.13	2.54	19	16.14	0.78	0.95
10	FStMa	no	6	H04	1	0	0	0	35	16.81	0.73	0.95
4	FVa	no	15	H08	1	0	0	0	20	13.90	0.71	0.90
15	ICo	yes	14	H06	1	0	0	0	20	9.15	0.61	0.81
16	IMa	no	17	H04	1	0	0	0	37	14.26	0.71	0.91
14	ISu	yes	14	H04, H07	2	0.14 ± 0.12	0.05 ± 0.04	0.29	27	7.53	0.63	0.80

Significant deviations from Hardy-Weinberg equilibrium (HWE) were detected in 36 of all 110 tests (at the Bonferroni corrected significance level of 0.45%). All populations showed at least two loci not in HWE and two loci displayed deviations from HWE in eight out of ten populations (Appendix 10). These deviations can be explained by a relatively high frequency of null alleles (Appendixes 10 & 11). Mean estimated null allele frequency per locus across populations ranged from 1.49 to 22.34%. Mean null allele frequency estimates per population across loci ranged from 8.13% (Susa) to 13.38% (Crau). All microsatellite analyses were additionally performed with a dataset excluding the four loci with the highest null allele

frequencies and with a dataset corrected for null allele presence. There were only slight quantitative and no qualitative differences compared to the analyses of the data set described below (results not shown).

Population genetic structure

At the mitochondrial level the overall fixation index of Φ_{ST} = 0.96 (P < 0.001) suggests a very strong differentiation between populations of *O. decorus*. Most population pairs were significantly different from each other except for some geographically close ones. Nonsignificant pairwise Φ_{ST} - value were found between the two Swiss populations (Ossona, Gampel) and Valbonne in Northern France. The differentiation between three populations located in the Camargue in France (Crau, Saint-Martin de Crau, Sisteron) was not significant, as well as the differentiation to the two Italian populations Susa in the North and Magredi in the East. High Φ_{ST} - values were found between all pairwise comparisons with Cogne from the Eastern lineage and with the population from Corsica (Piena, Table 4; Appendix 12). A very high amount of the variation (Φ_{CT} = 0.95; P < 0.0001) was explained when the following two groups were set in an AMOVA framework: the Italian populations from the Eastern lineage (Cogne) as one unit and the remaining populations from Switzerland, Italy and France as a second. The correlation between genetic and geographical distance for the entire data set was not significant (R^2 =0.00006; P = 0.42; Appendix 13A). The genetic relationships between populations from the Western lineage only did not support a pattern of isolation by distance (R^2 =0.00051; P = 0.39; Appendix 13B), nor while excluding the population from Corsica (R^2 =0.0101; P = 0.28; Appendix 13C).

Overall differentiation among populations in nucDNA was highly significant F_{ST} = 0.07 (P < 0.0001). All populations differed significantly from each other except for three populations located in the Camargue in France (Crau, Saint-Martin de Crau and Sisteron; Table 4). Pairwise F_{ST} ranged from 0.025 (between Crau and Valbonne) to 0.16 (between Gampel and Susa; all P-values < 0.0001). F_{ST} - values corrected for null allele presence were slightly lower, but nevertheless significant. The level of microsatellite differentiation between the two

geographically adjacent populations Gampel and Ossona (F_{ST} = 0.09; 29km distance) or Cogne and Susa (F_{ST} = 0.15; 60km distance) was much higher than between the two distant populations like Crau and Magredi (F_{ST} = 0.03; 625km distance). Consequently, microsatellite variability did not follow a pattern of IBD (R^2 = 0.021; P = 0.26) implicating that nuclear gene flow is not just explained by geographic distance (Appendix 13A). Within the Western lineage alone, the relationship between genetic and geographic distance was not significant either (R^2 = 0.00008; P = 0.48; Appendix 13B).

Table 4 Estimates of pairwise genetic differentiation among ten populations of *Oedaleus decorus*. Above the diagonal are pairwise Φ_{ST} - values for mtDNA. Below the diagonal are pairwise F_{ST} for nucDNA with corresponding values corrected for null allele presence in brackets. Population abbreviations are given in Table 3. All values are in percent. NS, nonsignificant; all other values have a significant P-value < 0.001 after Bonferroni correction.

	CHOs	CHOa	FCr	FPl	FSl	FStMa	FVa	ICo	IMa	ISu
CHOs	-	0.02 NS	87.50	94.73	47.84	79.44	1.83 NS	99.62	81.05	75.83
CHOa	9.33 (7.81)	-	76.97	97.11	51.88	100	0 NS	100	100	88.84
FCr	5.61 (3.84)	7.42 (6.03)	-	91.04	12.85 NS	-0.05 NS	76.68	99.24	3.07 NS	1.75 NS
FPl	7.73 (6.09)	9.51 (6.86)	2.34 (1.98)	-	57.39	94.62	96.89	99.62	95.61	93.87
FSl	6.03 (4.69)	7.10 (6.62)	0.91 (0.48) NS	2.99 (1.97)	-	5.31 NS	48.98	97.09	17.94 NS	14.07 NS
FStMa	7.16 (5.83)	7.49 (6.03)	0.69 (0.18) NS	2.76 (2.19)	1.31 (0.69) NS	-	100	100	0 NS	-0.07 NS
FVa	8.80 (8.73)	8.54 (8.94)	2.25 (1.85)	4.55 (3.44)	3.09 (2.09)	3.07 (2.32)	-	100	100	87.89
ICo	14.04 (11.11)	13.27 (11.11)	7.05 (5.81)	8.41 (7.17)	7.74 (6.07)	7.58 (6.16)	7.79 (6.80)	-	100	99.67
IMa	8.76 (6.72)	9.18 (7.51)	2.62 (1.88)	9.07 (2.57)	2.97 (2.05)	2.58 (1.88)	4.70 (3.59)	8.30 (6.42)	-	1.45 NS
ISu	16.52 (13.06)	16.10 (13.59)	8.59 (8.61)	10.70 (9.28)	9.42 (7.97)	8.57 (7.43)	12.45 (10.66)	16.31 (12.41)	9.25 (7.79)	-

Including all individuals from the ten populations, the first axis of the PCoA explained 23% and the second axis 18% of the total nucDNA variability, respectively. Two populations from Switzerland (Ossona, Gampel) and one population from Northern Italy (Susa) were clearly separated from each other (Figure 4). Bayesian clustering with Structure indicated that the most likely number of groups according to the modal value of the distribution of ΔK was three (Appendix 14). Examining the runs with K = 3 showed in six out of ten runs the following clusters: Switzerland, Susa (Italy) and a last cluster merging the remaining populations irrespective of their phylogenetic origin (Appendix 14A). In three runs, Cogne clustered with both Swiss populations (Appendix 14B) and in one run showed mixed ancestry with the

Swiss populations and the cluster encompassing French and Italian samples (Appendix 14C). If *K* was set to four, six runs revealed the following distinct groups: Switzerland, Susa, Cogne and a last cluster consisting of all French populations and Magredi (Appendix 14C). In three runs, STRUCTURE grouped Cogne with Gampel and in the remaining run with Ossona, resulting in a separation of the Swiss populations (Appendixes 14 D & E).

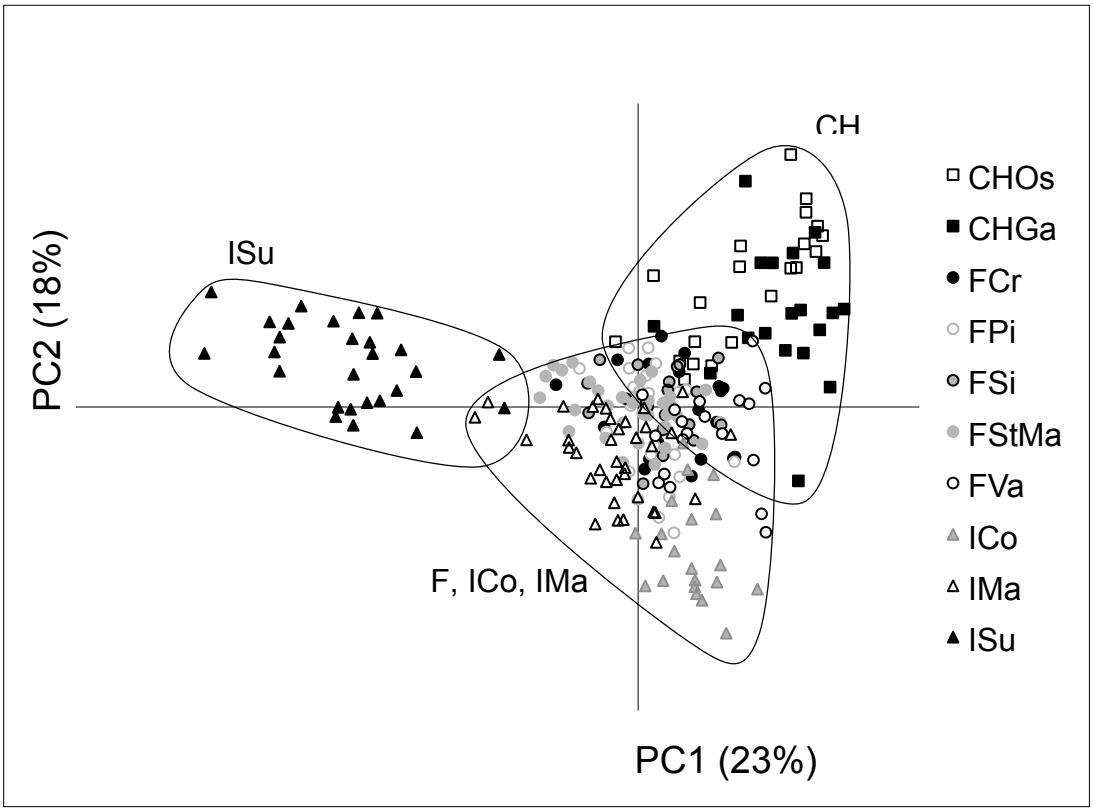

Fig. 4 Principal Coordinate Analysis (PCoA) using microsatellite genotypes of individuals from ten *Oedaleus decorus* populations. The first axis explains 23% and the second 18% of the total variability, respectively. Populations from the same country are shown by the same symbols: Switzerland (□), France (○) and Italy (△). Different fillings of the symbols indicate different populations. Population abbreviations are given in Table 3. Two populations from Switzerland and one population from Italy (Susa) were clearly separated from the others.

Discussion

Deep genetic divergence in Oedaleus decorus

The mtDNA data of *Oedaleus decorus* across its distribution range in Europe showed a deep genetic split with high nodal support into an Eastern and a Western lineage (Fig. 3). The net pairwise divergence between the two lineages of 6.9% (Table 2) is in the range of differentiation sometimes found between congeneric species, such as 5.4% between *Oedaleus asiaticus* and *Locusta migratoria* based on mitochondrial 16S rRNA (Yin *et al.*, 2008) and 14.2% based on the mitochondrial gene *COI* (Ma *et al.*, 2009). A similarly high divergence of the Western and the Eastern mtDNA lineage to *O. asiaticus* of 4.8% and 7.9% respectively, may point towards the existence of three distinct species or at least two subspecies within *O. decorus*. Although we did not calibrate the molecular clock for the two lineages in *O. decorus*, the estimated divergence time between *O. decorus* and *O. asiaticus* of 35Ma (Fries *et al.*, 2007) would suggest a rather historical split of the two lineages in *O. decorus*, largely predating the last glacial maximum. The presence of two lineages was additionally supported by phylogenetic analyses based on the mitochondrial gene *ND2* (Appendix 15). Several restrictions in the treatment with samples showing potential pseudogenes allowed us to verify the mitochondrial origin of the sequences which were included in the analyses. We can therefore confirm the authenticity of the deep genetic split into two lineages within *O. decorus* and rule out confounding influences of unknowingly coamplified nuclear copies.

Cytonuclear discordance in the suture-zone in northern Italy

If the mtDNA split into two lineages actually reflects the presence of “cryptic” species, individuals from either lineage should be reproductively isolated, but quite identical in their morphology. To date, an Eastern and a Western lineage within this species was unknown and no comparative morphological study between individuals from different localities across

Europe has been conducted so far. However, when focussing on the population in northern Italy (Cogne), we found a lack of congruence between mtDNA and microsatellite data. Individuals from the population in Cogne which are exclusively part of the Eastern mtDNA lineage did not reflect the deep mtDNA split at microsatellite loci. Instead, they most often clustered with genotypes originating from the Western mtDNA lineage (Appendix 14). This pattern represents a case of cytonuclear discordance and was observed in several species within mtDNA contact zones (Braaker & Heckel, 2009; Renoult *et al.*, 2009; Yang & Kenagy, 2009) Discrepancies between mtDNA and microsatellite loci can be explained by the different inheritance of both markers in combination with the retention of ancient polymorphisms at microsatellite loci. Historical separation could have been long enough for allopatric divergence at mitochondrial marker, but too short for the differentiation at microsatellite loci as a consequence of the four times higher effective population size at nucDNA compared to mtDNA (Renoult *et al.*, 2009; Yang & Kenagy, 2009). Although the ancient mtDNA split in *O. decorus* suggests complete lineage sorting of ancestral polymorphism, these inferences need to be verified with a dense multilocus data set and coalescent-based approaches (Yang & Kenagy, 2009). Alternatively, sex-biased dispersal could explain the discrepancies between mtDNA and microsatellite loci in the population in northern Italy. Male-biased dispersal was suggested in the temperate grasshopper *Chorthippus albomarginatus* (Walters *et al.*, 2006), and the smaller body size of males compared with females of *O. decorus* could support this behaviour (Baur *et al.*, 2006). Strong male-biased dispersal can lead to increased gene flow at microsatellite loci and to local admixing between the Eastern and Western lineage, but meanwhile preserve the phylogeographic mtDNA pattern (Braaker & Heckel, 2009; Yang & Kenagy, 2009). This scenario seems quite compatible with our results, but needs to be further investigated especially with a focus on the species' dispersal behaviour and the presence of Western haplotypes within the investigated population. As a last alternative, local introgression and the exchange of genes between two lineages may explain our results. Reported cases of introgressive hybridisation mostly involves mtDNA with varying levels of replacement (Alves

et al., 2008; Renoult *et al.*, 2009; Yang & Kenagy, 2009). Introgression between evolutionary lineages or species after secondary contact is promoted especially during changing environmental conditions. Theoretical models suggest that introgression almost exclusively occurs from a local species into the gene pool of the invading species (Currat *et al.*, 2008). The phenomenon is additionally enhanced when the invading species expands, thus leading to a very high frequency of the introgressed alien allele (Renoult *et al.*, 2009). If we assume the individuals from the Western mtDNA lineage as the invaders, the absence of Western mtDNA haplotypes would point towards a complete mitochondrial introgression from the local individuals which are part of the Eastern mtDNA lineage. This phenomenon, however, has been rarely reported (Nevado *et al.*, 2009) as it requires a high number of hybridisation events at the contact zone (Currat *et al.*, 2008). If we however take into account strong male-biased dispersal, males from the Western mtDNA lineage were the first to invade the range of local individuals from the Eastern mtDNA lineage and the admixing with resident females would be favoured (Alves *et al.*, 2008). As a consequence of strong male-biased dispersal, we expect less introgression at nucDNA markers compared to mtDNA markers (Petit & Excoffier, 2009). Further understanding of the processes which led to the cytonuclear discordance in *O. decorus*, however, would require an extensive sampling in the region of the suture-zone and the investigation of additional nuclear (sequence) loci.

Genetic variability and population outbreaks

The overall relative low variability in mtDNA markers (Table 3) may follow a classical gradient of diversity with decreasing latitude (Hewitt, 1999) or indicate low variability in the ancestral populations (Seddon *et al.*, 2001). Reduced genetic diversity in populations at the species' northern expansion limit as a consequence of long-range migration with subsequent founder events seems not unlikely (Hewitt, 1996; Ibrahim *et al.*, 1996). However, in order to confirm these assumptions, samples from southern regions across the species distribution range would be necessary. Microsatellite variability on the contrary was much higher than mtDNA

diversity. Because of the lower effective population size of mtDNA, founder effects and population bottlenecks affect genetic diversity at this marker more strongly than at microsatellite loci (Canestrelli *et al.*, 2006). In addition, population outbreaks with a strong male-bias could enhance diversity at microsatellite loci relative to mtDNA markers. Although swarming events were reported for *O. decorus* (Boczki, 2007; Harz, 1975; Schmidt & Lilge, 1996; Yin *et al.*, 2008), there is no information available about their frequencies and consequences on population structure. Chapuis *et al*. (2009) indicated that massive outbreaks in the locust *Locusta migratoria* are especially common in Asia, but less frequent in the Western distribution range of the species. The authors further suggested severe homogenising effects on the population structure as a consequence of enhanced gene flow during swarming events. If we assume a comparative scenario for *O. decorus*, male-biased outbreaks could enhance microsatellite diversity in local populations, but would allow population differentiation as long as these events are rather uncommon.

Phylogenetic analyses and their limitations

If we interpret our data in the context of the climatic oscillations during the Pleistocene, individuals from both mtDNA lineages most likely colonised their recent northern territories from southern regions. Based on the current genetic data in *O. decorus* we cannot identify those southern areas, but strengthen the potential importance of North Africa as an ecologically and climatically favourable region during the last glacial maximum. Although Fet (2007) and dry museum specimen collected for this study suggested the presence of the species in Africa, extensive sampling and molecular analyses are required to confirm the taxonomic status of the African individuals and their relationship to the European ones, respectively. In contrast to analogous studies, our analyses did not reveal a distinct Iberian lineage although the importance of this Peninsula as a refugial area for many taxa is known (Cooper *et al.*, 1995; Heuertz *et al.*, 2004; Paulo *et al.*, 2001; Schmitt & Seitz, 2004). The absence of the Iberian lineage may indicate the extinction of the species during the

glaciations (Taberlet *et al.*, 1998) or, however, be an artefact due to insufficient sampling across this Peninsula. Within the Western lineage a cluster consisting of the most northern population (Valbonne) and both populations in Switzerland and the separation of the Corsican population (Fig. 3) may indicate multiple Southern refugia or independent colonisation from a common refugium. But given the phylogenetic proximity of these haplogroups, the existence of multiple southern refugia seems rather unlikely. During the glaciations, large areas of Corsica were under ice-cover (Allen *et al.*, 2008) and so, the species most likely colonised the island post-glacially. The lowering of the Mediterranean Sea during the ice-age (Hewitt, 1999; Shackleton *et al.*, 1984) may have facilitated a colonisation from the European mainland, as shared haplotypes between samples from Sisteron (Southern France) and Corsica may indicate. However, we cannot rule out anthropogenic influences which may have transported individuals from Corsica to Sisteron or vice versa, and an additional colonisation from the geographically adjacent Italian west coast. Because the genetic relationship within the Western mtDNA lineage did not support a pattern of isolation by distance, nor while excluding the highly differentiated Corsican population, we concluded that the population structure is probably not driven by distance but rather by population specific demographic history.

We found evidence for significantly reduced microsatellite variability in populations inhabiting previously glaciated areas compared to populations from areas not affected by the last glacial maximum (Table 3). High mountains were not inhabitable during the LGM for a long time and therefore, the last places which were colonised after the retreat of the ice-cover; most probably from neighbouring populations. The reduced microsatellite diversity in the two Swiss populations and in the population from Susa may be a consequence of founder events and subsequent isolation with enhanced genetic drift.

Conclusion and Outlook

In this study we illustrate the potential of using both cytoplasmic and microsatellite marker to reveal complex patterns of cytonuclear discordance. The interpretation of mtDNA data alone would simply have revealed the existence of two highly divergent lineages in *O. decorus* with no admixing between them. On the other hand, microsatellite data would have obscured the evolutionary past of the population from the Eastern mtDNA lineage, but strengthen the separation of three populations within the Western lineage. Simply the combination of both markers made it possible to infer the complex pattern in the suture zone in northern Italy. For further studies it would be interesting to quantify the extent of cytonuclear discordance across the species range and to infer in more detail potential causes which may have led to the observed pattern. With the current genetic data only, it is difficult to answer whether the highly divergent lineages should be regarded as subdivisions, subspecies or cryptic species. Extensive sampling across the species' distribution range, additional nuclear (sequence) loci and morphological and behavioural data are needed. Different estimates of pairwise divergence between the same two species *Oedaleus asiaticus* and *Locusta migratoria* only due to different loci should advise caution in using such estimates for further inferences, as well in relying on estimates of divergence times which in the study of Fries *et al*. (Fries *et al.*, 2007) was based on single individuals. As the relationship between the two lineages in *O. decorus* and *O. asiaticus* could not be fully resolved, we suggest for further studies to enlarge sample sizes especially with a focus on *O. asiaticus* and to investigate additional markers.

Acknowledgements

I would like to thank Gerald Heckel for his excellent supervision, his ongoing support and for all the knowledge he shared during the last year. Furthermore, I would like to thank Raphaël Arlettaz for providing samples, for his knowledge about the study species and for the opportunity to go to Italy for sampling purposes.

I am grateful to Yang Liu for his constant support, good ideas and his deep interest in my study species and for his company in Italy. I would like to thank Martin C. Fischer for his helpful inputs and discussions during the last year. I am thankful to Tamara Hofer, Tania Jenkins, Lu Dong, Benjamin Peter, Andrea Jordan and Esther Schläpfer for their comments and inputs during the preparation of the manuscript. I would like to thank Andreas Gschwind and Susanne Tellenbach for their great company when sharing the office and all the other CMPG members for the good time.

Many thanks to Christian Schlüchter for his interesting inputs about the climatic conditions during the last ice-age and to Marcello Tagliavia for helpful comments when dealing with dry museum specimen. I'm grateful to Francesca Tami and Paolo Glerean for their assistance and help in Magredi.

I would like to thank the following people for providing valuable samples: Fabrizio Rigato, Mercedes Paris, Daniel Petit, Axel Hochkirch, Martin Schmid-Entling, Yang Liu, David Kieffer, Roberto Casalini, Leonardo Latella, Donato Mancini, Luca Bartolozzi, Martin Fikacek, Luc Willemse, Kelly Papapavlou, Mustafa Ünal, David Murany and Le Kang.

My special thanks go to my family and my friends for their unbelievable support, patience and understanding when running a bit late because of some lab issues. They all know what it meant to me.

References

Akaike H (1974) A new look at the statistical model identification. *IEEE Transactions on Automatic Control* **19**, 716-723.

Allen R, Siegert M, Payne A (2008) Reconstructing glacier-based climates of LGM Europe and Russia - Part 2: A dataset of LGM precipitation/temperature relations derived from degree-day modelling of palaeo glaciers. *Climatic Past*, 249-263.

Alves PC, Melo-Ferreira J, Freitas H, Boursot P (2008) The ubiquitous mountain hare mitochondria: multiple introgressive hybridization in hares, genus Lepus. *Philosophical Transactions of the Royal Society of London B* **363**, 2831-2839.

Arctander P (1995) Comparison of a mitochondrial gene and a corresponding nuclear pseudogene. *Proceedings of the Royal Society B: Biological Sciences* **262**, 13-19.

Baur B, Baur H, Roesti C, Roesti D, Thorens P (2006) *Die Heuschrecken der Schweiz* Haupt, Bern.

Bellmann H (2006) *Der Kosmos Heuschrecken Führer* Frankh-Kosmos, Stuttgart.

Bellmann H, Luquet GC (2009) *Guide de Sauterelles, Grillons et Criquets d'Europe occidentale*, Neuchâtel et Paris.

Bensasson D, Zhang DX, Hartl DL, Hewitt GM (2001) Mitochondrial pseudogenes: evolution's misplaced witnesses. *Trends in Ecology & Evolution* **16**, 314-321.

Bensasson D, Zhang DX, Hewitt GM (2000) Frequent assimilation of mitochondrial DNA by grasshopper nuclear genomes. *Molecular Biology and Evolution* **17**, 406-415.

Berg HM, Zuna-Kratky T (1997) *Heuschrecken und Fangschrecken (Insecta; Saltatoria, Mantodea). Rote Listen ausgewählter Tiergruppen Niederösterreichs* NÖ Landesregierung / Abt. Natuerschutz, Wien.

Berthier K, Loiseau A, Streiff R, Arlettaz R (2008) Eleven polymorphic microsatellite markers for *Oedaleus decorus* (Orthoptera, Acrididae), an endangered grasshopper in Central Europe. *Molecular Ecology Resources* **8**, 1363-1366.

Blanchard JL, Lynch M (2000) Organellar genes - why do they end up in the nucleus? *Trends in Genetics* **16**, 315-320.

Boczki R (2007) Erster sicherer Nachweis der Kreuzschrecke *Oedaleus deocrus* (Germar 1826), für Deutschland (Caelifera: Acrididae, Oedipodinae). *Articulata* **22**, 63-75.

Braaker S, Heckel G (2009) Transalpine colonisation and partial phylogeographic erosion by dispersal in the common vole (*Microtus arvalis*). *Molecular Ecology* **18**, 2518-2531.

Canestrelli D, Cimmaruta R, Costantini V, Nascetti G (2006) Genetic diversity and phylogeography of the Apennine yellow-bellied toad *Bombina pachypus*, with implications for conservation. *Molecular Ecology* **15**, 3741-3754.

Chapuis MP, Estoup A (2007) Microsatellite null alleles and estimation of population differentiation. *Molecular Biology and Evolution* **24**, 621-631.

Chapuis MP, Loiseau A, Michalakis Y*, et al.* (2009) Outbreaks, gene flow and effective population size in the migratory locust, *Locusta migratoria*: a regional-scale comparative survey. *Molecular Ecology* **18**, 792-800.

Cicconardi F, Nardi F, Emerson BC, Frati F, Fanciulli PP (2009) Deep phylogeographic divisions and long-term persistence of forest invertebrates (Hexapoda: Collembola) in the North-Western Mediterranean basin. *Molecular Ecology* **19**, 386-400.

Cooper SJB, Ibrahim KM, Hewitt GM (1995) Postglacial expansion and genome subdivision in the European grasshopper *Chorthippus parallelus*. *Molecular Ecology* **4**, 49-60.

Currat M, Ruedi M, Petit R, Excoffier L (2008) The hidden side of invasions: massive introgression by local genes. *Evolution* **62**, 1908-1920.

Defaut B, Sardet E, Braud Y (2009) *Orthoptera: Ensifera et Caelifera*, Dijon.

Evanno G, Regnaut S, Goudet J (2005) Detecting the number of clusters of individuals using the software Structure: a simulation study. *Molecular Ecology* **14**, 2611-2620.

Excoffier L, Smouse P, Quattro J (1992) Analysis of Molecular Variance inferred from metric distance among DNA haplotypes. Application to human mitochondrial DNA restriction data. *Genetics* **131**, 479-491.

Falush D, Stephens M, Pritchard JK (2003) Inference of population structure using multilocus genotype data: linked loci and correlated allele frequencies. *Genetics* **164**, 1567-1587.

Felsenstein J (2004) *Inferring Phylogenies.* Sinauer Associates., Sunderland, Massachusetts.

Fet V (2007) *Biogeography and Ecology of Bulgaria* Springer Netherlands.

Feulner PGD, Bielfeldt W, Zachos FE*, et al.* (2004) Mitochondrial DNA and microsatellite analyses of the genetic status of the presumed subspecies *Cervus elaphus montanus* (Carpathian red deer). *Heredity* **93**, 299-306.

Fink S, Excoffier L, Heckel G (2004) Mitochondrial gene diversity in the common vole *Microtus arvalis* shaped by historical divergence and local adaptations. *Molecular Ecology* **13**, 3501-3514.

Fries M, Chapco W, Contreras D (2007) A molecular phylogenetic analysis of the Oedipodinae and their intercontinental relationships. *Journal of Orthoptera Research* **16**, 115-125.

Gomboc S, Trontelj P (2001) *Analiza stanja in Ogrozenosti biotske raznovrstnosti ravnokrilcev s smernicami za izboljsanje stanja* Natural History Museum Ljubliana, Ljubliana.

Goudet J (2001) FSTAT, a program to estimate and test gene diversities and fixation indices (version 2.9.3). Available from http://www.unil.ch/izea/softwares/fstat.html. Updated from Goudet (1995).

Gu X, Fu YX, Li WH (1995) Maximum likelihood estimation of the heterogeneity of substitution rate among nucleotide sites. *Molecular Biology and Evolution* **12**, 546-557.

Hall TA (1999) BioEdit: a user-friendly biological sequence alignment editor and analysis program for Windows 95/98/NT. *Nucleic Acids Symposium Series* **41**, 95-98.

Harz K (1975) *Die Orthopteren Europas II*, The Hague.

Heckel G, Burri R, Fink S, Desmet JF, Excoffier L (2005) Genetic structure and colonization processes in European populations of the common vole *Microtus arvalis*. *Evolution* **59**, 2231-2242.

Herterich K (1991) *Modelling the palaeo-climate* Fischer, Stuttgart.

Heuertz M, Fineschi S, Anzidei M*, et al.* (2004) Chloroplast DNA variation and postglacial recolonization of common ash (*Fraxinus excelsior*) in Europe. *Molecular Ecology* **13**, 3437-3452.

Hewitt GM (1996) Some genetic consequences of ice ages, and their role in divergence and speciation. *Biological Journal of the Linnean Society* **58**, 247-276.

Hewitt GM (1999) Post-glacial re-colonization of European biota. *Biological Journal of the Linnean Society* **68**, 87-112.

Hewitt GM (2000) The genetic legacy of the Quaternary ice ages. *Nature* **405**, 907-913.

Hewitt GM (2004) Genetic consequences of climatic oscillations in the Quaternary. *Philosophical Transactions of the Royal Society of London B* **359**, 183-195.

Holm S (1979) A simple sequentially rejective multiple test procedure. *Scandinavian Journal of Statistics* **6**, 65-70.

Holuša J, Kočárek P (2005) *Red List of Threatened Species in the Czech Republic. Invertebrates, Orthoptera* Agentura ochrany ptirody a krajiny CR, Prague.

Huelsenbeck JP, Ronquist F (2001) MrBayes: a program for the Bayesian inference of phylogeny. *Bioinformatics* **17**, 754-755.

Ibrahim KM, Nichols RA, Hewitt GM (1996) Spatial patterns of genetic variation generated by different forms of dispersal during range expansion. *Heredity* **77**, 282-291.

Ingrisch S, Köhler G (1998) *Die Heuschrecken Mitteleuropas* Westarp-Wissenschaften, Magdeburg.

Kaltenbach A (1970) *Zusammensetzung und Herkunft der Orthopterenfauna im pannonischen Raum Österreich* Annalen des Naturhistorischen Museums in Wien, Wien.

Kimura M (1980) A simple method for estimating evolutionary rates of base substitution through comparative studies of nucleotide sequences. *Journal of Molecular Evolution* **16**, 111-120.

Kočárek P, Holuša J, Vidlicka L (1999) Check-list of Blattaria, Mantodea, Orthoptera and Dermaptera of the Czech and Slovak Republics. *Articulata* **14**, 177-184.

Kotlik P, Deffontaine V, Mascheretti S*, et al.* (2006) A northern glacial refugium for bank voles (*Clethrionomys glareolus*). *Proceedings of the National Academy of Sciences of the USA* **103**, 14860-14864.

Krystufek B, Bryia J, Buzan E (2009) Mitochondrial phylogeography of the European ground squirrel, *Spermophilus citellus*, yields evidence on refugia for steppic taxa in the southern Balkans. *Heredity* **103**, 129 - 135.

Kumar S, Tamura K, Nei M (2004) MEGA3: integrated software for molecular evolutionary genetics analysis and sequence alignment. *Briefings in Bioinformatics* **5**, 150-163.

Librado P, Rozas J (2009) DnaSP v5: a software for comprehensive analysis of DNA polymorphism data. *Bioinformatics* **25**, 1451.

Ma C, Liu C, Yang P, Kang L (2009) The complete mitochondrial genomes of two band-winged grasshoppers, *Gastrimargus marmoratus* and *Oedaleus asiaticus*. *BMC Genomics* **10**, 156.

Monnerat C, Thorens P, Walter T, Gonseth Y (2007) *Rote Liste der Heuschrecken der Schweiz* Bundesamt für Umwelt, Bern und Schweizer Zentrum für die Kartographie der Fauna, Neuenburg.

Nevado B, Koblm, Ller S*, et al.* (2009) Complete mitochondrial DNA replacement in a Lake Tanganyika cichlid fish. *Molecular Ecology* **18**, 4240-4255.

Page RDM (1996) TreeView: an application to display phylogenetic trees on personal computers. *Bioinformatics* **12**, 357.

Paulo OS, Dias C, Bruford MW, Jordan WC, Nichols RA (2001) The persistence of Pliocene populations through the Pleistocene climatic cycles: Evidence from the phylogeography of an Iberian lizard. *Proceedings of the Royal Society B-Biological Sciences* **268**, 1625-1630.

Peakall ROD, Smouse PE (2006) GenAlEx 6: genetic analysis in Excel. Population genetic software for teaching and research. *Molecular Ecology Notes* **6**, 288-295.

Petit R, Excoffier L (2009) Gene flow and species delimitation. *Trends in Ecology & Evolution* **24**, 386-393.

Posada D (2008) jModelTest: phylogenetic model averaging. *Molecular Biology and Evolution* **25**, 1253.

Pritchard JK, Stephens M, Donnelly P (2000) Inference of population structure using multilocus genotype data. *Genetics* **155**, 945-959.

R Development Core Team (2009) *R: a language and environment for statistical computing*. In: *R foundation for statistical computing*, Vienna.

Rambaut A, Drummod A (2007) Tracer v.1.4, Available from http://beast.bio.ed.ac.uk/Tracer.

Ray N, Adams JM (2001) A GIS-based vegetation map of the world at the Last Glacial Maximum (25,000-15,000 BP). *Internet Archaeology* **11**, 1-44.

Renoult J, Geniez P, Bacquet P, Benoit L, Crochet P (2009) Morphology and nuclear markers reveal extensive mitochondrial introgressions in the Iberian Wall Lizard species complex. *Molecular Ecology* **18**, 4298-4315.

Ritchie J (1981) A taxonomic revision of the genus Oedaleus Fieber (Orthoptera: Acrididae). *Bulletin of the British Museum* **42**, 83-183.

Ronquist F, Huelsenbeck JP (2003) MrBayes 3: Bayesian phylogenetic inference under mixed models. *Bioinformatics* **19**, 1572.

Rosenberg NA (2004) Distruct: a program for the graphical display of population structure. *Molecular Ecology Notes* **4**, 137-138.

Rousset F (1997) Genetic differentiation and estimation of gene flow from F-statistics under isolation by distance. *Genetics* **145**, 1219-1228.

Saitou N, Nei M (1987) The neighbour joining method: a new method for reconstructing phylogenetic trees. *Molecular Biology and Evolution* **4**, 406-425.

Sambrook J, Fritsch EF, Maniatis T (1989) *Molecular Cloning: a Laboratory Manual.* Cold Spring Harbor Laboratory Press, Cold Spring Harbor, New York.

Schmidt GH, Lilge R (1996) *Geographische Verbreitung der Oedipodinae (Orthopteroidea, Caelifera, Acrididae) in Europa und Randgebieten* Verlag Dr. Kovac, Hamburg.

Schmitt T (2007) Molecular biogeography of Europe: Pleistocene cycles and postglacial trends. *Frontiers in Zoology* **4**, 11.

Schmitt T, Giessel A, Seitz A (2003) Did *Polyommatus icarus* (Lepidoptera: Lycaenidae) have distinct glacial refugia in southern Europe? Evidence from population genetics. *Biological Journal of the Linnean Society* **80**, 529-538.

Schmitt T, Seitz A (2004) Low diversity but high differentiation: the population genetics of *Aglaope infausta* (Zygaenidae: Lepidoptera). *Journal of Biogeography* **31**, 137-144.

Schweizer M, Excoffier L, Heckel G (2007) Fine-scale genetic structure and dispersal patterns in the common vole *Microtus arvalis*. *Molecular Ecology* **16**, 2463-2473.

Seddon JM, Santucci F, Reeve NJ, Hewitt GM (2001) DNA footprints of European hedgehogs, *Erinaceus europaeus* and *E. concolor*: Pleistocene refugia, postglacial expansion and colonization routes. *Molecular Ecology* **10**, 2187-2198.

Shackleton JC, Andel THV, Runnels CN (1984) Coastal paleogeography of the Central and Western Mediterranean during the last 125,000 years and its archaeological implications. *Journal of Field Archaeology* **11**, 307-314.

Song H, Buhay J, Whiting M, Crandall K (2008) Many species in one: DNA barcoding overestimates the number of species when nuclear mitochondrial pseudogenes are coamplified. *Proceedings of the National Academy of Sciences of the USA* **105**, 13486-13491.

Taberlet P, Fumagalli L, Wust-Saucy AG, Cosson J (1998) Comparative phylogeography and postglacial colonization routes in Europe. *Molecular Ecology* **7**, 453-464.

Tami F, Fontana P (2002) Gli Ortotteroidei dei Magredi del torrente Cellina (Friuli-Venezia Giulia, Italia nord-orientale). *Atti del Museo Friulano di Storia Naturale* **24**, 115-146.

Tamura K, Nei M (1993) Estimation of the number of nucleotide substitutions in the control region of mitochondrial DNA in humans and chimpanzees. *Molecular Biology and Evolution* **10**, 512-526.

Tavaré S (1986) Some probabilistic and statistical problems on the analysis of DNA sequences. *Lectures of Mathematical Life Science* **17**, 57-86.

Tavaré S, Balding DJ, Griffiths RC, Donnelly P (1997) Inferring coalescence times from DNA sequence data. *Genetics* **145**, 505-518.

Thompson JD, Gibson TJ, Plewniak F, Jeanmougin F, Higgins DG (1997) The CLUSTAL_X windows interface: flexible strategies for multiple sequence alignment aided by quality analysis tools. *Nucleic Acids Research* **25**, 4876.

Ustinova J, Achmann R, Cremer S, Mayer F (2006) Long repeats in a huge genome: microsatellite loci in the grasshopper *Chorthippus biguttulus*. *Journal of Molecular Evolution* **62**, 158-167.

Walters RJ, Hassall M, Telfer MG, Hewitt GM, Palutikof JP (2006) Modelling dispersal of a temperate insect in a changing climate. *Proceedings of the Royal Society B-Biological Sciences* **273**, 2017-2023.

Yang D, Kenagy G (2009) Nuclear and mitochondrial DNA reveal contrasting evolutionary processes in populations of deer mice (*Peromyscus maniculatus*). *Molecular Ecology* **18**, 5115-5125.

Yin XC, Li XJ, Wang WQ*, et al.* (2008) Phylogenetic analyses of some genera in Oedipodidae (Orthoptera: Acridoidea) based on 16S mitochondrial partial gene sequences. *Insect Science* **15**, 471-476.

Zhang DX, Hewitt GM (1996a) Highly conserved nuclear copies of the mitochondrial control region in the desert locust *Schistocerca gregaria*: some implications for population studies. *Molecular Ecology* **5**, 295-300.

Zhang DX, Hewitt GM (1996b) Nuclear integrations: challenges for mitochondrial DNA markers. *Trends in Ecology & Evolution* **11**, 247-251.

Appendix 1

Map of all available *Oedaleus decorus* and *Oedaleus asiaticus* samples across their distribution ranges in Europe, Northern Africa and Central-Asia, respectively. Many samples could not be included in the study as either DNA extraction or subsequent amplification of dry museum specimen failed. Even amplification with internal primers and adapted PCR protocols did not improve this, most probably due to fragmentation of the DNA and pigments or chemicals blocking amplification or sequencing reactions. Numbers are cross-referenced with Table 1 and 2 in Appendix 2.

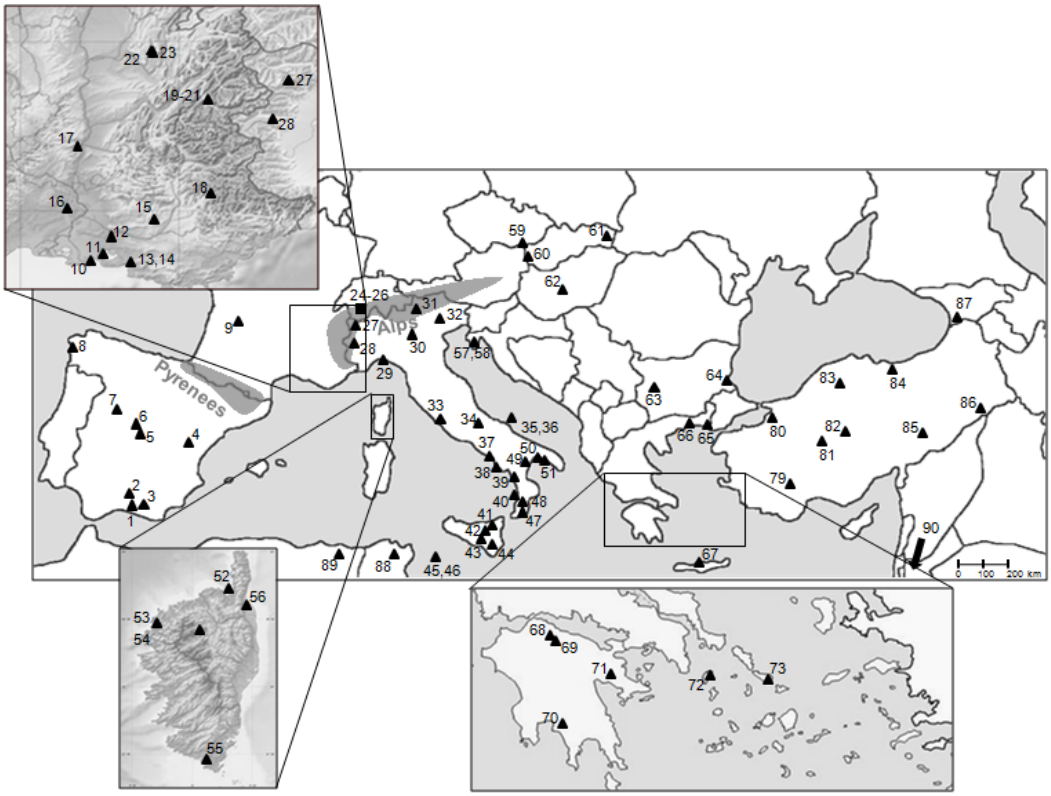

Appendix 2

Sampling locations of *Oedaleus decorus* in Europe and Northern Africa. Map reference numbers are listed as shown in the upper figure in Appendix 1. Given are sampling site (country, location, label, coordinates), the collection date, the number of samples and the initials of the people who provided the specimen. Museum specimen are indicated with stars. R (Raphaël Arlettaz, University of Berne), FR (Fabrizio Rigato, Museo Civicio di Storia Naturale, Milano), MP (Mercedes Paris, Museo nacional de Ciencias Naturales, Madrid), D (Daniel Petit, France), A (Axel Hochkirch, University of Trier), MS (Martin Schmid-Entling, University of Berne), E (Eveline Kindler, Yang Liu, David Kieffer, Berne), C (Roberto Casalini, Rome), LL (Leonardo Latella, Museo di Verona), FE (Francesca Tami, Udine), DM(Donato Mancini, Portici), B (Luca Bartolozzi, Florence), MF (Martin Fikacek, Prague), LW (Luc Willemse, Leiden), K (Kelly Papapavlou, Athens), MU (Mustafa Ünal, Bölümü), MD (David Murany, Budapest).

Map.ref	Country	Location	Label	Latitude	Longitude	sampling date	*n*	donor
1	Spain	Sierra Nevada, Capileira	ECa	36°57'N	03°21'W	01.09.2007	33	R
2*	Spain	Granada, Puerto de la Mora	EPu	37°17'N	03°27'W	19.07.1965	2	FR
3*	Spain	Laujar, Almería	ELa	36°59'N	02°53'W	unknown	1	MP
4*	Spain	Teruel	ETe	40°20'N	01°06'W	unknown	1	MP
5*	Spain	Brunete	EBr	40°24'N	03°59'W	unknown	1	MP
6*	Spain	Cercedilla, Estación Alpina	ECe	40°44'N	04°03'W	unknown	1	MP
7*	Spain	Negrilla, Salamance	ENe	41°05'N	05°35'W	unknown	1	MP
8*	Spain	La Toja, Pontevedra	ETo	42°29'N	08°51'W	unknown	1	MP
9*	France	La Rochebeaucourt-et-Argentine	FRoA	45°29'N	00°23'E	31.07.1998	1	D
10*	France	Etang des Aulnes / Crau	FEt	43°35'N	04°48'E	29.08.2005	1	A
11*	France	Vergières / Crau	FVe	43°34'N	04°49'E	29.08.2005	1	A
12*	France	Grand Lubéron	FLu	43°47'N	05°13'E	28.08.1996	1	D
13	France	St. Martin de Crau	FStMa	43°34'N	04°50'E	02.07.2009	35	MS
14*	France	Bouches du Rhône, Crau	FCr	43°35'N	05°18'E	05.09.2005	20	R
15*	France	Saumane	FSa	44°05'N	05°41'E	27.08.1999	1	D
16*	France	St. Alexandre / Rhône	FAx	44°14'N	04°38'E	29.08.2005	1	A
17*	France	Saint-Ilpize à St. Marcel	FMa	45°11'N	03°23'E	03.09.2002	1	D
18	France	Sisteron	FSi	44°11'N	05°56'E	05.09.2005	20	R
19	France	Briançonnais, La Roche-de-Rame	FRo	44°45'N	06°34'E	07.09.2005	3	R
20	France	Briançonnais, L'Argentière-la-Bessée	FAr	44°47'N	06°33'E	07.09.2005	11	R
21	France	Briançonnais, Saint-Martin de Queyrières	FSt	44°50'N	06°35'E	06.09.2005	6	R
22	France	Ain,Lyon, Valbonne	FVa	45°52'N	05°07'E	17.08.2008	20	R
23*	France	Blyes, à Port Galland	FBl	45°51'N	05°15'E	12.07.2003	1	D
24	Switzerland	Hérémence, Combioula	CHCo	46°10'N	07°24'E	29.08.2005	8	R
25	Switzerland	St-Martin, Ossona	CHOs	46°10'N	07°25'E	06.08.2005	13	R
26	Switzerland	Gampel	CHGa	46°18'N	07°44'E	18. - 25.08.2005	20	R
27	Italy	Basse Valle di Cogne	ICo	45°36'N	07°22'E	31.08.2005	20	R
28	Italy	Susa	ISu	45°08'N	07°02'E	18.07.2009	30	E
29*	Italy	Caffarella	ICa	44°31'N	08°50'E	19.08.1945	2	C
30	Italy	Veneto, Verona, Villafranca	IVi	45°21'N	10°50'E	07.1946	2	LL/FR
31*	Italy	Trentino, Merano	IMe	46°40'N	11°09'E	01.08.1952	1	FR
32	Italy	Udine, Magredi di cordenons	IMa	46°04'N	12°44'E	08. - 13.09.2009	38	FE
33*	Italy	Lazio, Montefiascone	IMo	42°32'N	12°02'E	20.09.1946	1	FR
34*	Italy	Capo Pescara, Popoli	IPo	42°10'N	13°49'E	25.08.1992	1	FR
35*	Italy	Isola Tremiti, San Nicola	ISN	42°07'N	15°30'E	09.1954/1955	4	FR
36*	Italy	Isola Capraia	ICa	42°08'N	15°30'E	24.06.1955	2	FR
37*	Italy	Campania, Sessa Aurunca	ISa	41°14'N	13°56'E	24.08.1936	1	DM
38*	Italy	Campania, Battipaglia	IBa	40°36'N	14°58'E	19.07.1940	1	DM
39*	Italy	Campania, Capaccio	ICa	40°25'N	15°04'E	24.06.1947	1	DM
40*	Italy	Cetraro, Calabria	ICe	39°31'N	15°56'E	07.1948	2	LL
41*	Italy, Sicily	Rocca di Novara	IRN	38°02'N	15°05'E	03.09.1967	2	FR
42*	Italy, Sicily	Randazzo, Etna	IRa	37°52'N	14°57'E	07.08.1969	2	FR
43*	Italy, Sicily	Geraci, Sicuto	IGe	37°51'N	14°09'E	06.1967	1	LL
44*	Italy, Sicily	Bronte, Monto Rossa, Etna	IBr	37°47'N	14°50'E	09.06.1985	1	FR

continued

Map.ref	Country	Location	Label	Latitude	Longitude	sampling date	*n*	donor
45*	Italy, Sicily	Isola di Lampedusa, Cala Galera	ICg	35°30'N	12°35'E	15.07.1993	1	B
46*	Italy, Sicily	Isola di Lampedusa, Capo Peneto	ICp	35°30'N	12°35'E	08.10.1969	3	FR
47*	Italy	Caulonia, Monte Gremi	IGr	38°22'N	16°24'E	14.09.1948	2	FR
48*	Italy	Nicastro	INi	38°58'N	16°19'E	29.07.1905	1	DM
49*	Italy	Basilicata	IBa	40°38'N	15°58'E	14.07.1975	1	B
50*	Italy	Puglia, river Fortore	IFo	40°47'N	17°06'E	unknown	1	B
51*	Italy	Puglia, Taranto	ITa	40°28'N	17°14'E	unknown	2	DM
52*	France, Corse	St Florent	FFl	42°40'N	09°18'E	05.07.2005	1	D
53*	France, Corse	Argentella	FAr	42°27'N	08°40'E	30.07.2007	1	D
54	France, Corse	Piana, Capo Rossa	FPi	42°14'N	08°38'E	12.07.2006	24	R
55*	France, Corse	Figari	FFi	41°29'N	09°07'E	24.07.2006	1	D
56*	France, Corse	Bastia	FBa	42°42'N	09°27'E	08.08.2007	1	D
57	Croatia	Krk, Voz	HRVo	45°13'N	14°34'E	15.09.2005	12	R
58	Croatia	Krk, Obzovo	HROb	44°58'N	14°45'E	15.09.2005	9	R
59*	Czech Republic	Kyjov	CZKy	49°00'N	17°07'E	unknown	1	MF
60*	Slovenia	Sekule	SLOSe	48°36'N	17°00'E	06.08.1055	1	FR
61*	Slovakia	Somotor	SKSo	48°24'N	21°49'E	22.07.1951	2	MF
62*	Hungary	Fülöphaza	HFü	46°53'N	19°25'E	07.09.1977	2	MD
63*	Bulgaria	Petrich	BGPe	41°23'N	23°12'E	10.08.1960	4	MF
64*	Bulgaria	Michurin	BGMi	42°10'N	27°50'E	05.08.1962	1	MF
65*	Greece	Thraki, Evros delta, Dadia	GRDa	41°07'N	26°13'E	02.07.200	1	LW
66*	Greece	Nea Karvali	GRNk	40°57'N	24°30'E	27.06.2008	3	LW
67*	Greece	Crete	GRCr	35°14'N	24°48'E	01.06.1934	1	MF
68*	Greece	Achaia, Skepasto	GRSk	38°04'N	22°04'E	26.07.2005	1	LW
69*	Greece	Kalavrita	GRKa	38°01'N	22°06'E	28.07.2005	1	LW
70*	Greece	Pelop. Taygetos Mts. Topista (Anogeia)	GRTa	37°00'N	22°18'E	22.07.1971	1	LW
71*	Greece	Argolis, Mt Artemisio	GRArg	37°39'N	22°51'E	24.07.2008	1	LW
72*	Greece	Tzia Island, Vorukari-Otzias	GRTz	37°36'N	24°18'E	13.06.2005	1	LW
73*	Greece	Cyclades Isls, Tinos	GRTi	37°32'N	25°09'E	31.07.2005	1	LW
74*	Greece	Anidros	GRAn	37°24'N	26°29'E	24.06.1997	1	K
75*	Greece	Lira	GRLir	37°16'N	26°46'E	31.05 - 24.6 1997	1	K
76*	Greece	Lipsos	GRLip	37°18'N	26°45'E	13. - 14.07 1997	1	K
77*	Greece	Arkioi	GRAr	37°23'N	26°44'E	23.06.1997	1	K
78*	Greece	Komoros	GRKo	37°24'N	26°43'E	18.06.1997	1	K
79*	Turkey	Akgol-Lake	TAk	37°39'N	29°45'E	08.08.1906	1	MD
80*	Turkey	Bursa	TBu	40°11'N	29°04'E	unknown	1	MD
81*	Turkey	Sivrihisar	TSv	39°27'N	31°32'E	25.08.1969	2	FR
82*	Turkey	Ankara	TAn	39°52'N	32°49'E	1930	2	MF
83	Turkey	Çankırı	TCa	40°50'N	32°45'E	29.08.2009	1	MU
84*	Turkey	Gölköy	TGö	40°37'N	37°32'E	24.06.1953	2	MF
85*	Turkey	between Silvas & Malatya	TSi	38°20'N	38°18'E	08.1957	1	LL
86*	Turkey	Bürücek	TBü	37°22'N	42°09'E	31.07.1947	1	MF
87*	Georgia	Adjar	GeAd	41°40'N	42°12'E	18.06.1957	1	MF
88*	Algeria	El Guerrah	AEg	36°08'N	06°36'E	15.09.1979	1	FR
89*	Egypt	Cairo	EgCa	30°03'N	31°14'E	unknown	1	FR
90*	Tunis	Kairouan	TuKa	35°40'N	10°06'E	29.05.1930	2	MF

Sampling locations of *Oedaleus decorus* and *Oedaleus asiaticus* in Eastern Europe and Central Asia, respectively. Map reference numbers are listed as shown in the lower figure in Appendix 1. Given are sampling site (country, location, label, coordinates), the collection date, the number of samples and the initials of the people who provided the specimens. Museum specimens are indicated with stars. Y (Yang Liu, University of Berne), L (Le Kang, Beijing), MF (Martin Fikacek, Prague), MD (David Murany, Budapest).

Map.ref	Country	Location	Label	Latitude	Longitude	sampling date	*n*	donor
1*	Russia	Stawropol	OdecRSt	45°03'N	41°59'E	unknown	1	MF
2	Russia	Kurgan	OdecRKur	54°37'N	64°27'E	15.06.2009	5	Y
3*	Kazakhstan	Imantav	OdecKIm	52°58'N	68°21'E	04.09.1962	2	MD
4*	Kazakhstan	Ili	OdecKIl	43°52'N	77°04'E	1954/57	2	MD
5*	Kazakhstan	Almaty	OdecKAl	43°16'N	76°53'E	07.1955/58	5	MD
6*	Kazakhstan	Tscharin	OdecKTs	43°15'N	78°54'E	10.07.1959	12	MD
7*	Mongolia	Ulaangom	OdecMUl	49°59'N	92°04'E	07.07.1968	2	MD
8*	Mongolia	Bayannuur	OdecMBa	47°49'N	104°26'E	24.07.1968	1	MD
9*	Mongolia	Lün	OdecMLu	47°51'N	105°15'E	25.07.1968	3	MD
10*	Mongolia	Zogt-Ovoo	OdecMZo	44°25'N	105°19'E	09.07.1967	3	MD
11*	Mongolia	Baruun Bayan-Ulaan	OdecMBar	45°10'N	101°25'E	22.08.1966	1	MF
12*	Mongolia	Dalanzadgad	OdecMDa	43°34'N	104°25'E	24.08.1966	2	MF
13*	Mongolia	Dariganga	OdecMDar	45°18'N	113°50'E	06.08.1965	1	MD
14*	Mongolia	Mörön	OdecMMo	47°22'N	110°19'E	28.07.1965	2	MD
15*	Mongolia	Delgerkhangai	OdecMDe	45°14'N	104°48'E	11.07.1967	11	MD
16*	Mongolia	Dashinchilen	OdecMDas	47°51'N	104°02'E	23.07.1968	20	MD
17*	Mongolia	Undur Khan	OdecMUn	47°19'N	110°39'E	30.07.1965	1	MD
18*	China	Xilinhot	OasCNXi	43°56'N	116°03'E	07.2008	3	L

Appendix 3

Overview of all primer combinations used in this study. Given are the name of each primer, its function (forward or reverse primer), the length in base-pair, melting points based on two different calculations, the annealing temperature at which optimal amplification was achieved in this study, its sequence and remarks. Primer pairs, which led to a successful amplification, are highlighted in grey.

Primer name	Primer type	Length	Melting points	optimal Ta	Sequence
Odec_dloop_F1	Forward	20bp	51.3 / 54.2 °C	55 °C	**5'**-TGGCACGAAATATGCCAATA-**3'**
Odec_dloop_R1	Reverse	20bp	55.4 / 54.7 °C		**5'**-TGGGGTATGAACCCATTAGC-**3'**
Odec_dloop_R2	Reverse	27bp	50.4 / 49.2 °C		**5'**-TTTCTTCTATTGTGGTAAATTTTTGTT-**3'**
Odec_dloop_R3	Reverse	26bp	55.0 / 56.4 °C	55 °C	**5'**-CATTTAACTGAATGTAAGACCCATAC-**3'**

Primer name	Primer type	Length	Melting points	optimal Ta	Sequence
Odec_dloop_F1	Forward	20bp	51.3 / 54.2 °C	55 °C	**5'**-TGGCACGAAATATGCCAATA-**3'**
Odec_dloop_int_R1	Intern Reverse	20bp	55.4 / 48.6 °C	52 °C	**5'**-GGTTTGCGGGATATGTGTTC-**3'**

Primer name	Primer type	Length	Melting points	optimal Ta	Sequence
Odec_dloop_int_F1	Intern Forward	20bp	55.4 / 66.6 °C	52° C	**5'**-GAACACATATCCCGCAAACC-**3'**
Odec_dloop_R3	Reverse	26bp	55.0 / 56.4 °C	55 °C	**5'**-CATTTAACTGAATGTAAGACCCATAC-**3'**

Primer name	Primer type	Length	Melting points	optimal Ta	Sequence
Odec_ND2_F1	Forward	23bp	54.2 / 51.0 °C	50 °C	**5'**-TGAGATGCCTGAATAAAGGGTTA-**3'**
Odec_ND2_R1	Reverse	20pb	55.4 / 48.9 °C	50 °C	**5'**-AGGGTGCCAATGTCCTTATG-**3'**

Appendix 4

PCR reaction mix for different molecular analyses. Given are the analyses method, the reaction ingredients, their concentration if necessary and their amount.

Amplification of *ctr* fragment (600bp)	
H_20	12.50 µl
dNTP	4.80 µl
Primer 1 (10pmol/µl)	1.00 µl
Primer 2 (10pmol/µl)	1.00 µl
$MgCl_2$ (25mM)	1.00 µl
10 x buffer incl. 15mM $MgCl_2$	2.50 µl
Taq polymerase (QIAGEN)	0.20 µl
DNA	2.00 µl
End volume	**25.00 µl**

Sequencing of *ctr* fragment (600bp)	
H_20	4.00 µl
Primer (10pmol/µl)	1.00 µl
BigDye v.3.1 (diluted)	2.50 µl
DNA	2.50 µl
End volume	**10.00 µl**

Amplification of *ctr* fragment (200bp) 1st round	
H_20	12.50 µl
dNTP	4.80 µl
Primer 1 (10pmol/µl)	1.00 µl
Primer 2 (10pmol/µl)	1.00 µl
$MgCl_2$ (25mM)	1.00 µl
10 x buffer incl. 15mM $MgCl_2$	2.50 µl
Taq polymerase (QIAGEN)	0.20 µl
DNA	2.00 µl
End volume	**25.00 µl**

Amplification of *ctr* fragment (200bp) 2nd round	
H_20	13.50 µl
dNTP	4.80 µl
Primer 1 (10pmol/µl)	1.00 µl
Primer 2 (10pmol/µl)	1.00 µl
$MgCl_2$ (25mM)	1.00 µl
10 x buffer incl. 15mM $MgCl_2$	2.50 µl
Taq polymerase (QIAGEN)	0.20 µl
PCR product	**1.00 µl**
End volume	**25.00 µl**

Sequencing of *ctr* fragment (200bp)	
H_20	2.50 µl
Primer (10pmol/µl)	1.00 µl
BigDye v.3.1 (diluted)	2.50 µl
DNA	4.00 µl
End volume	**10.00 µl**

Multiplex sets 1 and 2	
PCR Multiplex-Mix QIAGEN	5.00 µl
H_20 bidest	3.00 µl
Primer-Mix	1.00 µl
DNA	1.00 µl
End volume	**10.00 µl**

Individual loci repetition	
H_20	6.10 µl
dNTP	0.30 µl
Primer 1 (10pmol/µl)	0.20 µl
Primer 2 (10pmol/µl)	0.20 µl
$MgCl_2$ (25mM)	0.00 µl
10 x buffer incl. 15mM $MgCl_2$	1.00 µl
Taq polymerase (QIAGEN)	0.20 µl
DNA	2.00 µl
End volume	**10.00** µl

Amplification of *ND2 fragment* (1040bp)	
H_20	12.50 µl
dNTP	4.80 µl
Primer 1 (10pmol/µl)	1.00 µl
Primer 2 (10pmol/µl)	1.00 µl
$MgCl_2$ (25mM)	1.00 µl
10 x buffer incl. 15mM $MgCl_2$	2.50 µl
Taq polymerase (QIAGEN)	0.20 µl
DNA	2.00 µl
End volume	**25.00 µl**

Sequencing of *ND2* fragment (1040bp)	
H_20	4.00 µl
Primer (10pmol/µl)	1.00 µl
BigDye v.3.1 (diluted)	2.50 µl
DNA	2.50 µl
End volume	**10.00 µl**

Appendix 5

Cycling conditions for different molecular analyses. Given are the analyses methods and for each step the temperature, the time and the number of cycles.

Amplification of *ctr* fragment (600bp)			
Initial denaturation	95 °C	2 min	
Denaturation	94 °C	30 sec	35x
Annealing	55 °C	1 min	
Extension	72 °C	1 min	
Final extension	72 °C	10 min	

Sequencing of *ctr* fragment (600bp)			
Initial denaturation	96 °C	50 sec	
Denaturation	96 °C	10 sec	35x
Annealing	50 °C	10 sec	
Extension	60 °C	4.5 min	

Amplification of *ctr* fragment (200bp)			
Initial denaturation	95 °C	2 min	
Denaturation	94 °C	30 sec	40x
Annealing	52 °C	1 min	
Extension	72 °C	1 min	
Final extension	72 °C	10 min	

Sequencing of *ctr* fragment (200bp)			
Initial denaturation	96 °C	50 sec	
Denaturation	96 °C	10 sec	35x
Annealing	50 °C	10 sec	
Extension	60 °C	4.5 min	

Multiplex sets 1 and 2			
Taq activation	95 °C	15 min	
Denaturation	94 °C	30 sec	30x
Annealing	57 °C	1.5 min	
Extension	72 °C	1 min	
Final extension	60 °C	30 min	

Individual loci repetition			
Initial denaturation	94 °C	5 min	
Denaturation	94 °C	1 min	30x
Annealing	53 °C	1 min	
Extension	72 °C	1.25 min	
Final extension	72 °C	10 min	

Amplification of *ND2* fragment (1040bp)			
Initial denaturation	95 °C	2 min	
Denaturation	94 °C	30 sec	35x
Annealing	50 °C	1 min	
Extension	72 °C	1 min	
Final extension	72 °C	10 min	

Sequencing of *ND2* fragment (1040bp)			
Initial denaturation	96 °C	50 sec	
Denaturation	96 °C	10 sec	35x
Annealing	50 °C	10 sec	
Extension	60 °C	4.5 min	

Appendix 6

Compilation of 11 microsatellite loci used in this study. Set 1 (bold), Set2 (italic). The colours correspond to the fluorescent labels of the forward primers: red (ATTO565), green (Yakima Yellow), blue (6-FAM) and yellow (ATTO550). Ranges of the primers are based on genotyping results in this study and are listed in detail in the table below.

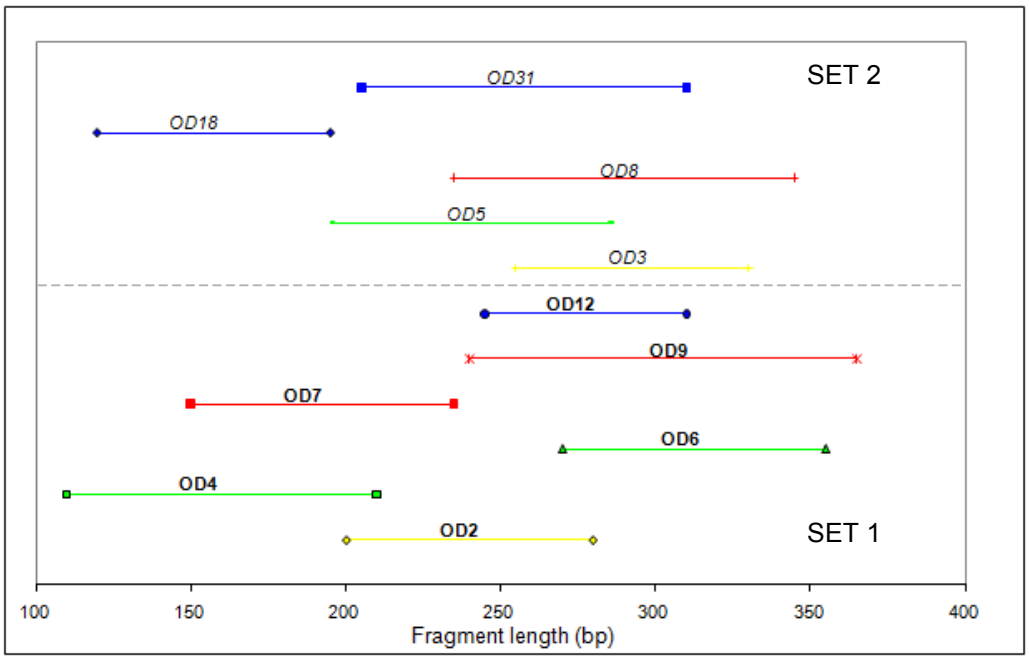

Characteristics of 11 microsatellite loci used in this study. For each primer its name, dye and range in base-pair are shown.

Primer	Colour	Range min	Range max	
OD2	ATTO550	200	330	Set 1
OD4	Yakima Yellow	110	260	
OD6	Yakima Yellow	250	400	
OD7	ATTO565	130	250	
OD9	ATTO565	160	380	
OD12	6-FAM	245	310	
OD3	ATTO550	210	340	Set 2
OD5	Yakima Yellow	110	285	
OD8	ATTO565	210	345	
OD18	6-FAM	120	200	
OD31	6-FAM	205	310	

Appendix 7

Primer mix concentrations for the two multiplex sets. Concentrations are mentioned for forward and reverse primers separately.

Set1

Primer-Mix	Colour	for 1 µl µl [100 µM]
OD2_F	ATTO550	0.02
OD2_R		0.02
OD4_F	Yakima Yellow	0.02
OD4_R		0.02
OD6_F	Yakima Yellow	0.02
OD6_R		0.02
OD7_F	ATTO565	0.02
OD7_R		0.02
OD9_F	ATTO565	0.02
OD9_R		0.02
OD12_F	6-FAM	0.02
OD12_R		0.02
Sum [µl]		0.24
dH_2O		0.76
Sum total [µl]		1

Set2

Primer-Mix	Colour	for 1 µl µl [100 µM]
OD3_F	ATTO550	0.02
OD3_R		0.02
OD5_F	Yakima Yellow	0.02
OD5_R		0.02
OD8_F	ATTO565	0.02
OD8_R		0.02
OD18_F	6-FAM	0.02
OD18_R		0.02
OD31_F	6-FAM	0.02
OD31_R		0.02
Sum [µl]		0.2
dH_2O		0.8
Sum total [µl]		1

Appendix 8A

The 38 variable sites of 376bp mtDNA observed among 178 *Oedaleus decorus* samples. The distribution of the haplotypes is illustrated in detail in Appendix 9A.

```
HO1 TTAGACTTAC TTAGTAATTT GGAGACTACT GTATTTTG
HO2 .........A .......... .......... ........
HO3 .......... .......... .......... ....CC..
HO4 A.GAGTC.T. .C.T..TCCC AAGAGTCT.C T.TCC.CA
HO5 A.GAGTC.T. .C.T..TCCC AAGAGTCT.C T.TCC..A
HO6 A.GAGTC.T. .C.T..TCCC AAGAGTCT.C T.T.C.CA
HO7 A.GAGTC.T. .CTT..TCCC AAGAGTCT.C T.TCC.CA
HO8 A.GAGTC.T. .C.TC.TCCC AAGAGTCT.C TCTCC.CA
HO9 A.GAGTC.T. .C.TC.TCCC AAGAGTCT.C TCT.CC.A
H10 A.GAGTC.T. .C.T..TCCC AAGAGTCT.C T.T.CC.A
H11 A.GAGTC.T. .C.TC.TCCC AAGAGTCT.C T.TCC.CA
H12 A.GAGTC.T. .C.C..TCCC AAGAGTCT.C T.TCC.CA
H13 A.GAGTCCT. .C.T..TCCC AAGAGTCT.C T.TCC.CA
H14 A.GAGTC.T. CC.T..TCCC AAGAGTCT.C T.TCC.CA
H15 A.GAGTC.T. .CTT..TCCC AAGAGTCTAC T.TCC.CA
H16 A.GAGTC.T. .C.T.TTCCC AAGAGTCT.C ..T.CC.A
H17 A.GAGTC.T. .C....TCCC AAGAGTCT.C ..T.CC.A
H18 .C........ .......... .......... ........
```

Appendix 8B

The 50 variable sites of 546bp mtDNA observed among 173 *Oedaleus decorus* samples. The distribution of the haplotypes is illustrated in detail in Appendix 9B.

```
HO1 TAGACTTACT TAGTATTTGG AGACTACTGT ATTTTGGAGA CTATGTACGA
HO2 ........A. .......... .......... .......... ..........
HO3 .......... .......... .......... ..CC...... ..........
HO4 AGAGTC.T.. C.T.TCCCAA GAGTCT.CT. TCC.CAAGAG TCTCT.T..G
HO5 AGAGTC.T.. C.T.TCCCAA GAGTCT.CT. TCC..AAGAG TCTCT.T..G
HO6 .......... .......... .......... .......... .......T..
HO7 AGAGTC.T.. C.T.TCCCAA GAGTCT.CT. TCC.CAAGAG TC.CT.T...
HO8 AGAGTC.T.. C.T.TCCCAA GAGTCT.CT. TCC.CAAGAG TCTCT.T.TG
HO9 AGAGTC.T.. C.T.TCCCAA GAGTCT.CT. T.C.CAAGAG TCTCT.T.TG
H10 AGAGTC.T.. CTT.TCCCAA GAGTCT.CT. TCC.CAAGAG TCTCT.T..G
H11 AGAGTC.T.. C.TCTCCCAA GAGTCT.CTC TCC.CAAGAG TCTCTCT..G
H13 AGAGTC.T.. C.T.TCCCAA GAGTCT.CT. T.CC.AAGAG TCTCT.T..G
H14 AGAGTC.T.. C.TCTCCCAA GAGTCT.CT. TCC.CAAGAG TCTCT.T..G
H15 AGAGTC.T.. C.C.TCCCAA GAGTCT.CT. TCC.CAAGAG TCTCT.T..G
H16 AGAGTCCT.. C.T.TCCCAA GAGTCT.CT. TCC.CAAGAG TCTCT.T..G
H17 AGAGTC.T.C C.T.TCCCAA GAGTCT.CT. TCC.CAAGAG TCTCT.T..G
H18 AGAGTC.T.. CTT.TCCCAA GAGTCTACT. TCC.CAAGAG TCTCT.T..G
H12 AGAGTC.T.. C.TCTCCCAA GAGTCT.CTC T.CC.AAGAG TCTCTCT..G
```

Appendix 9A

Distribution of the 18 haplotypes found in 178 *Oedaleus decorus* samples genotyped at 376bp mtDNA. Haplotype H04 is the most common haplotype and found in 14 populations located in Spain, Italy, Switzerland and France. Given are population and haplotype identification, as well as the frequency of a certain haplotype per population.

Haplotype	H01	H02	H03	H04	H05	H06	H07	H08	H09	H10	H11	H12	H13	H14	H15	H16	H17	H18
HRVo	**3**	**2**	0	0	0	0	0	0	0	0	0	0	0	0	0	0	0	0
HROb	**2**	0	**1**	0	0	0	0	0	0	0	0	0	0	0	0	0	0	0
ECa	0	0	0	**4**	**1**	0	0	0	0	0	0	0	0	0	0	0	0	0
EBr	0	0	0	0	0	0	0	0	0	**1**	0	0	0	0	0	0	0	0
ICo	**14**	0	0	0	0	0	0	0	0	0	0	0	0	0	0	0	0	0
ISu	0	0	0	**14**	0	0	0	0	0	0	0	0	0	0	0	0	0	0
IMa	0	0	0	**17**	0	0	0	0	0	0	0	0	0	0	0	0	0	0
IRa	0	0	0	0	0	0	0	0	0	0	0	0	0	0	0	0	0	0
IRN	0	0	0	0	0	0	0	0	0	0	0	0	0	0	0	**1**	0	0
CHOs	0	0	0	**18**	0	**2**	0	0	0	0	0	0	0	0	0	0	**1**	0
CHGa	0	0	0	**17**	0	0	0	0	0	0	0	0	0	0	0	0	0	0
FRo	0	0	0	**1**	0	0	0	0	0	0	0	0	0	0	0	0	0	0
FAr	0	0	0	**5**	0	0	0	0	0	0	0	0	0	0	0	0	0	0
FSt	0	0	0	**4**	0	0	**1**	0	0	0	0	0	0	0	0	0	0	0
FVa	0	0	0	**15**	0	0	0	0	0	0	0	0	0	0	0	0	0	0
FSi	0	0	0	**7**	0	0	**1**	**1**	**2**	**1**	**1**	**1**	0	0	0	0	0	0
FCr	0	0	0	**11**	0	0	**1**	0	0	0	0	0	**1**	**1**	**1**	0	0	0
FPi	0	0	0	0	0	0	0	**1**	**12**	0	0	0	0	0	0	0	0	0
FFl	0	0	0	0	0	0	0	0	**1**	0	0	0	0	0	0	0	0	0
FMa	0	0	0	**1**	0	0	0	0	0	0	0	0	0	0	0	0	0	0
FVe	0	0	0	**1**	0	0	0	0	0	0	0	0	0	0	0	0	0	0
FStMa	0	0	0	**6**	0	0	0	0	0	0	0	0	0	0	0	0	0	0
GRNk	0	0	0	0	0	0	0	0	0	0	0	0	0	0	0	0	0	**1**
TCa	**1**	0	0	0	0	0	0	0	0	0	0	0	0	0	0	0	0	0
RKur	**1**	0	0	0	0	0	0	0	0	0	0	0	0	0	0	0	0	0
Total	5	1	1	14	1	1	3	2	3	2	1	1	1	1	1	1	1	1

Appendix 9B

Distribution of the 18 haplotypes found in 173 *Oedaleus decorus* samples genotyped at 546bp mtDNA. Haplotype H04 is the most common haplotype and found in 11 populations located in Spain, France, Italy and Switzerland. Given are population and haplotype identification, as well as the frequency of a certain haplotype per population.

Haplotype	H01	H02	H03	H04	H05	H06	H07	H08	H09	H10	H11	H12	H13	H14	H15	H16	H17	H18
HRVo	**3**	**2**	0	0	0	0	0	0	0	0	0	0	0	0	0	0	0	0
HROb	**2**	0	**1**	0	0	0	0	0	0	0	0	0	0	0	0	0	0	0
ECa	0	0	0	**4**	**1**	0	0	0	0	0	0	0	0	0	0	0	0	0
ICo	0	0	0	0	0	**14**	0	0	0	0	0	0	0	0	0	0	0	0
ISu	0	0	0	**13**	0	0	**1**	0	0	0	0	0	0	0	0	0	0	0
IMa	0	0	0	**17**	0	0	0	0	0	0	0	0	0	0	0	0	0	0
CHOs	0	0	0	**1**	0	0	0	**17**	**2**	0	0	0	0	0	0	0	0	0
CHGa	0	0	0	0	0	0	0	**17**	0	0	0	0	0	0	0	0	0	0
FRo	0	0	0	**1**	0	0	0	0	0	0	0	0	0	0	0	0	0	0
FAr	0	0	0	**5**	0	0	0	0	0	0	0	0	0	0	0	0	0	0
FSt	0	0	0	**4**	0	0	0	0	0	**1**	0	0	0	0	0	0	0	0
FVa	0	0	0	**7**	0	0	0	**15**	0	0	0	0	0	0	0	0	0	0
FSi	0	0	0	**11**	0	0	0	0	0	**1**	**1**	**2**	**1**	**1**	**1**	0	0	0
FCr	0	0	0	0	0	0	0	0	0	**1**	0	0	0	0	0	**1**	**1**	**1**
FPi	0	0	0	0	0	0	0	0	0	0	**1**	**12**	0	0	0	0	0	0
FFl	0	0	0	0	0	0	0	0	0	0	0	**1**	0	0	0	0	0	0
FMa	0	0	0	0	0	0	0	**1**	0	0	0	0	0	0	0	0	0	0
FVe	0	0	0	**1**	0	0	0	0	0	0	0	0	0	0	0	0	0	0
FStMa	0	0	0	6	0	0	0	0	0	0	0	0	0	0	0	0	0	0
RKur	**1**	0	0	0	0	0	0	0	0	0	0	0	0	0	0	0	0	0
Total	3	1	1	11	1	1	1	4	1	3	2	3	1	1	1	1	1	1

Appendix 10

Characteristics of 11 microsatellite loci used in this study. Given is the number of samples (*N*), the number of alleles, observed (H_O) and expected (H_E) heterozygosity and the null allele frequency in percent. High values are coloured in green, low values in red, respectively.

	OD2	OD4	OD6	OD7	OD9	OD12	OD3	OD5	OD8	OD18	OD31	Min	Max	Mean
N	231	237	221	233	223	240	209	239	239	241	240	209	241	231
Number of alleles	53	54	48	41	59	29	31	39	52	36	41	29	59	43.923
H_O	0.671	0.789	0.480	0.815	0.673	0.792	0.397	0.469	0.833	0.859	0.867	0.397	0.867	0.685
H_E	0.961	0.952	0.940	0.952	0.968	0.947	0.938	0.934	0.958	0.944	0.956	0.934	0.968	0.950
Null allele frequency %	10.674	4.608	21.479	3.971	12.434	4.974	22.342	20.345	2.993	1.487	1.679	1.487	22.342	10.062

Characteristics of ten populations used for STR analyses. Given is the number of alleles, the number of alleles with a frequency higher than 5%, observed (H_O) and expected heterozygosity and (H_E) and the null allele frequency in percent. High values are coloured in green, low values in red, respectively.

Populati on	CHOs	CHGa	FCr	FPi	FSi	FStMa	FVa	ICo	IMa	ISu	Min	Max	Mean
Mean number of alleles	12.182	9.000	18.909	19.364	18.727	25.273	16.182	10.182	21.909	8.909	8.909	25.273	16.064
Mean number of alleles Freq. >=5%	5.909	6.727	10.636	5.909	9.636	6.091	7.545	6.727	7.000	5.545	5.545	10.636	7.173
H_O	0.623	0.671	0.668	0.772	0.778	0.727	0.713	0.612	0.713	0.632	0.612	0.778	0.691
H_E	0.815	0.799	0.926	0.901	0.923	0.938	0.878	0.792	0.902	0.780	0.780	0.938	0.865
Mean null allele frequency %	11.697	8.439	13.376	7.721	7.577	10.719	8.287	11.108	10.208	8.127	7.577	13.376	9.726

Results of tests for deviation from Hardy-Weinberg equilibrium (HWE) for each population and locus separately. *P* - values displaying significant deviations from HWE after Bonferroni correction are highlighted in green (adjusted significance level 0.45%). In addition, the total number of populations not in HWE per locus and the total number of loci not in HWE per populations is shown.

Populati on	CHOs	CHGa	FCr	FPi	FSi	FStMa	FVa	ICo	IMa	ISu	number of pop not in HWE
OD2	0.001	0.189	0.001	0.008	0.048	0.000	0.017	0.448	0.001	0.884	**4**
OD4	0.409	0.961	0.581	0.038	0.246	0.564	0.027	0.619	0.121	0.343	0
OD6	0.000	0.000	0.000	0.005	0.003	0.000	0.001	0.008	0.000	0.000	**8**
OD7	0.003	0.450	0.274	0.487	0.236	0.032	0.121	0.003	0.343	0.806	2
OD9	0.005	0.004	0.004	0.412	0.006	0.000	0.629	0.000	0.039	0.000	**5**
OD12	0.004	0.259	0.083	0.306	0.065	0.076	0.132	0.000	0.093	0.683	2
OD3	0.000	0.088	0.000	0.000	0.034	0.000	0.001	0.004	0.000	0.000	**8**
OD5	0.001	0.000	0.008	0.000	0.000	0.000	0.006	0.031	0.026	0.005	**5**
OD8	0.779	0.963	0.129	0.245	0.348	0.000	0.224	0.820	0.691	0.119	1
OD18	0.410	0.698	0.299	0.812	0.486	0.000	0.328	0.540	0.927	0.621	1
OD31	0.040	0.116	0.053	0.806	0.678	0.391	0.343	0.816	0.419	0.064	0
number of loci not in HWE	**6**	**3**	**4**	**2**	**2**	**7**	**2**	**4**	**3**	**3**	

Appendix 11

Estimated null allele frequencies per locus and population calculated with FREENA.

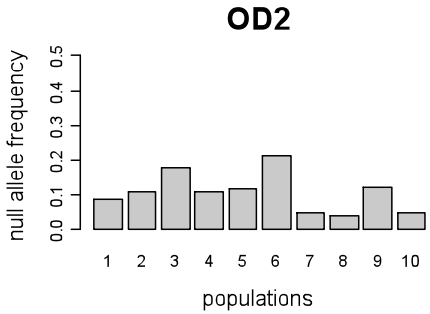

Appendix 12

Unrooted NJ trees of linearized pairwise Φ_{ST} - values and F_{ST} among ten populations based on mitochondrial and microsatellite loci, respectively. As the values are much greater for mtDNA than for microsatellite loci, the scales are not the same.

mtDNA

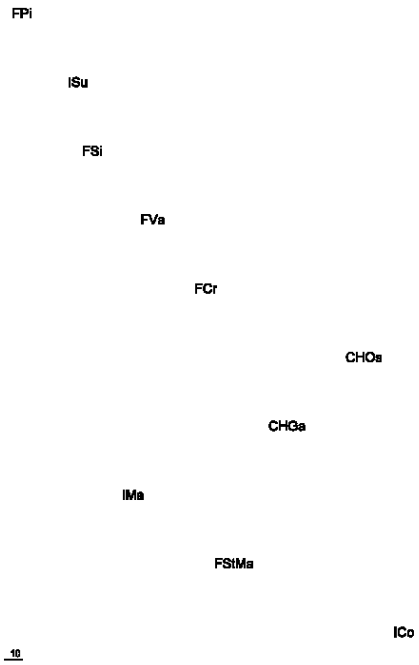

nucDNA

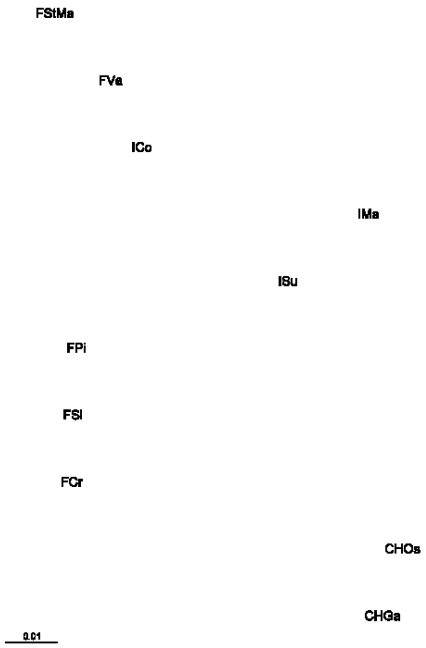

Appendix 13A

mtDNA

Correlation between matrices of geographic distances in log kilometres and pairwise linearized Φ_{ST} - values to test for isolation by distance (IBD) among ten populations. Significance was assessed by Mantel tests using 999 permutations. MtDNA variability does not follow a pattern of IBD. *P* - value = 0.42, y = -4.329x +116.5, R^2 = 0.00006.

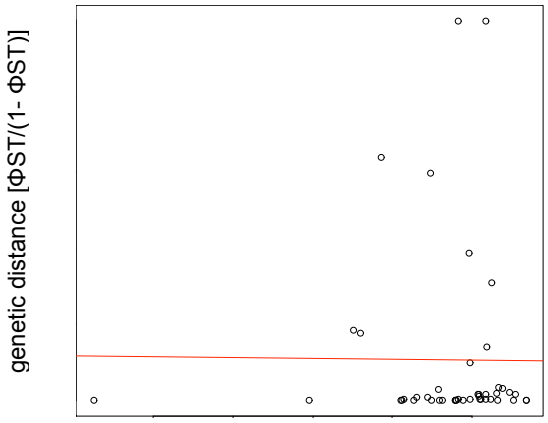

STRs

Correlation between matrices of geographic distances in log kilometres and linearized pairwise F_{ST} values to test for isolation by distance (IBD) among ten populations. Significance was assessed by Mantel tests using 999 permutations. STR variability does not follow a pattern of IBD. *P* - value = 0.26, y = -0.0152x + 0.115, R^2 = 0.0205.

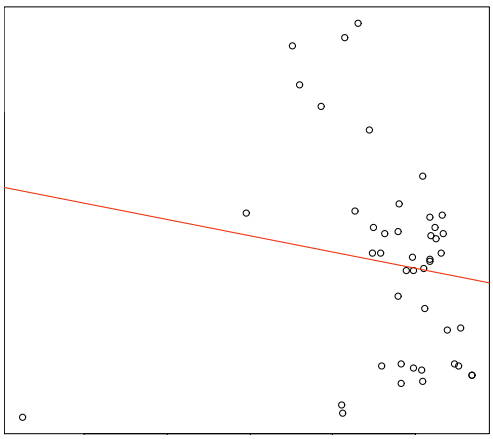

Appendix 13B

mtDNA excluding the population from the Eastern lineage (ICo)

Correlation between matrices of geographic distances in log kilometres and pairwise linearized Φ_{ST} - values to test for isolation by distance (IBD) among nine populations. Significance was assessed by Mantel tests using 999 permutations. MtDNA variability does not follow a pattern of IBD. *P* - value = 0.39, y = 34.977x – 21.76, R^2 = 0.0051.

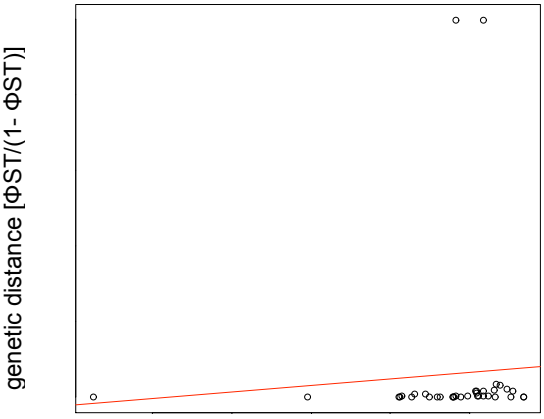

STRs excluding the population from the Eastern lineage (ICo)

Correlation between matrices of geographic distances in log kilometres and linearized pairwise F_{ST} values to test for isolation by distance (IBD) among nine populations. Significance was assessed by Mantel tests using 999 permutations. STR variability does not follow a pattern of IBD. *P* - value = 0.48, y =0.0009x + 0.069, R^2 = 0.00008.

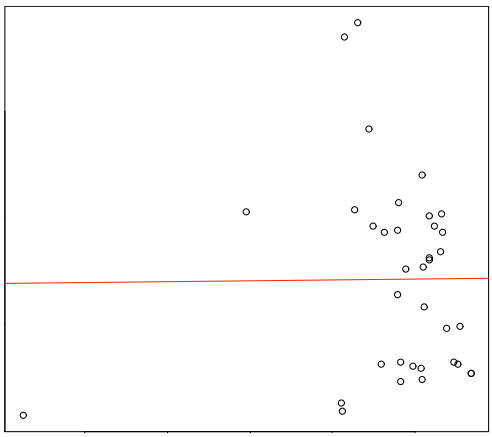

Appendix 13C

mtDNA excluding the population from Corsica

Correlation between matrices of geographic distances in log kilometres and pairwise linearized Φ_{ST} - values o test for isolation by distance (IBD) among eight populations. Significance was assessed by Mantel tests using 999 permutations. MtDNA variability does not follow a pattern of IBD. *P* - value = 0.28, y = 50.66x – 43.51, R^2 = 0.0101.

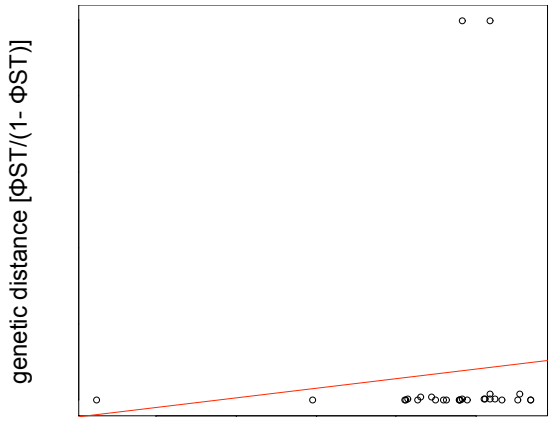

STRs excluding the population from Corsica

Correlation between matrices of geographic distances in log kilometres and linearized pairwise F_{ST} values to test for isolation by distance (IBD) among eight populations. Significance was assessed by Mantel tests using 999 permutations. STR variability does not follow a pattern of IBD. *P* - value = 0.35, y =0.0049x + 0.0636, R^2 = 0.0028.

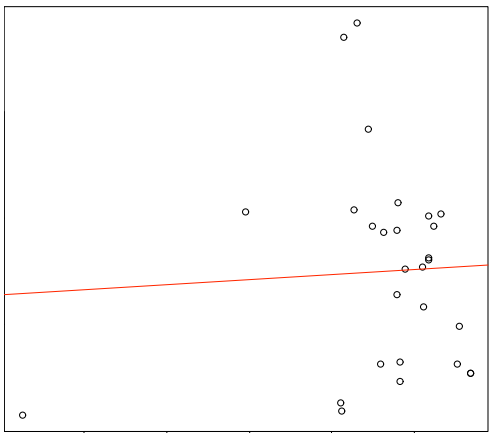

Appendix 14

The program STRUCTURE was used to assign individuals to populations and the most likely number of clusters (*K*) was defined following the approach suggested by Evanno *et al*. (2005). The mean likelihood L (*K*) over 10 runs was plotted for each *K* (a) and the absolute values of the differences between successive values of L' (*K*) were calculated (b). Finally, Δ*K* was estimated as the mean of the absolute values of L'' (*K*) averaged over 10 runs and divided by the standard deviation of L (*K*) (c). Dividing by the standard deviation takes into account the increasing variance with increasing *K*. Once the optimal *K* is reached, following L (*K*) should plateau or only slightly increase, which would result in *K* = 4 in this case. An additional indication of the true *K* is the modal value of the distribution of Δ*K* and would suggest three genetic clusters.

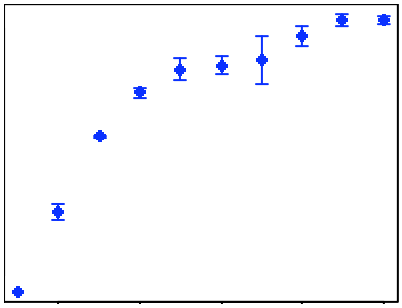

(a)

(b)

(c)

Different clustering with *K* = 3. Each vertical bar corresponds to one individual. The labels above the figure indicate the country of origin for each population. The label below displays the name of the population. The colour indicates the membership according to STRUCTURE. The number in brackets shows how often a certain pattern was found within ten iterations.

A (6x)

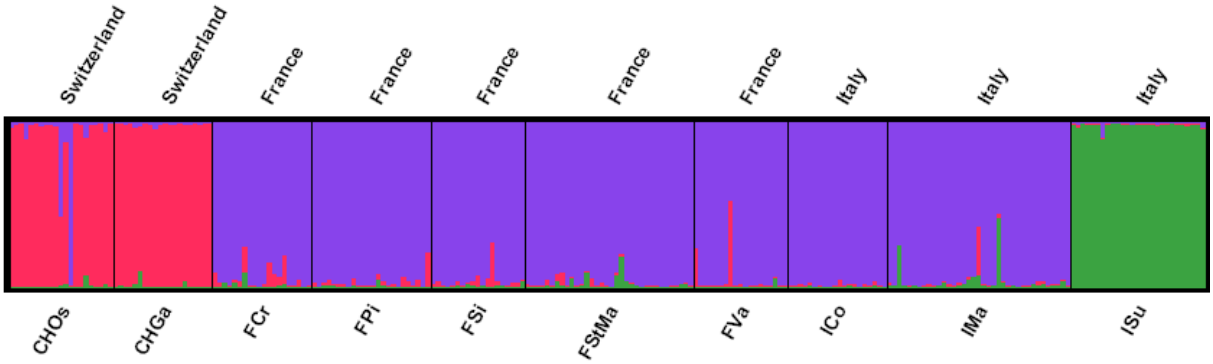

B (3x)

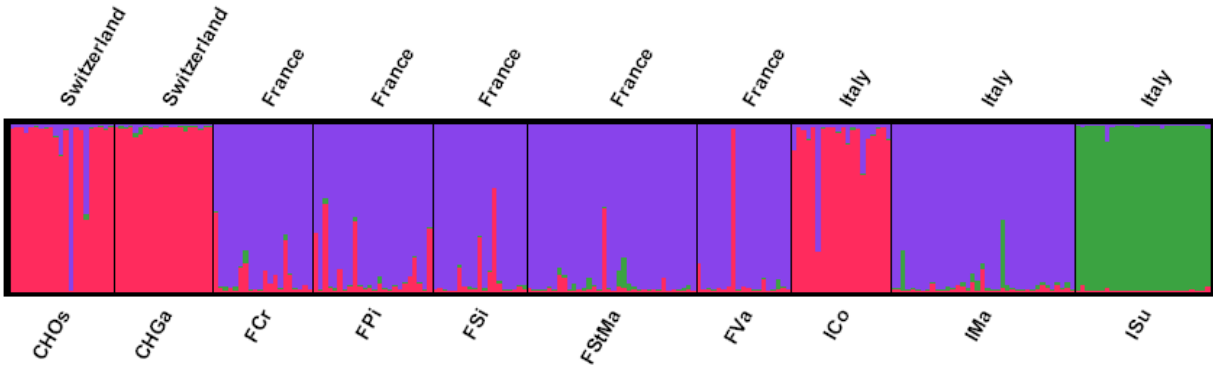

C (1x)

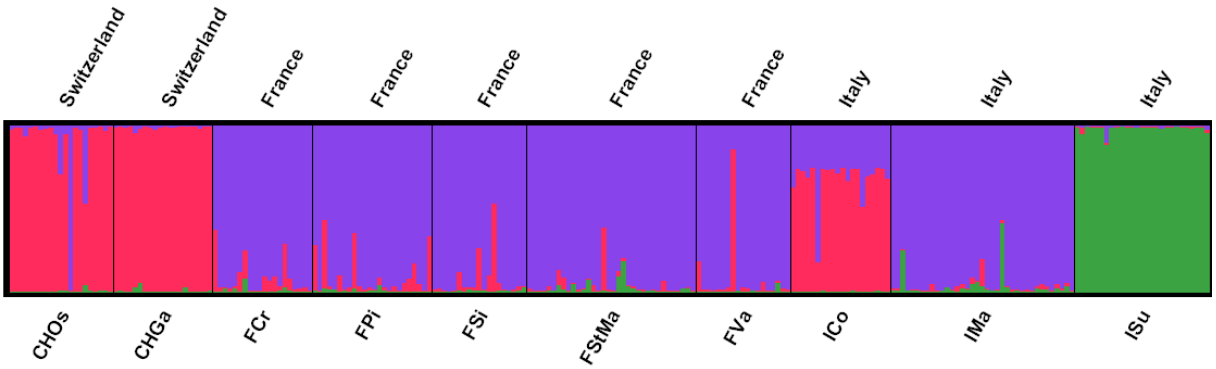

Different clustering with *K* = 4. Each vertical bar corresponds to one individual. The labels above the figure indicate the country of origin for each population. The label below displays the name of the population. The colour indicates the membership according to STRUCTURE. The number in brackets shows how often a certain pattern was found within ten iterations.

C (6x)

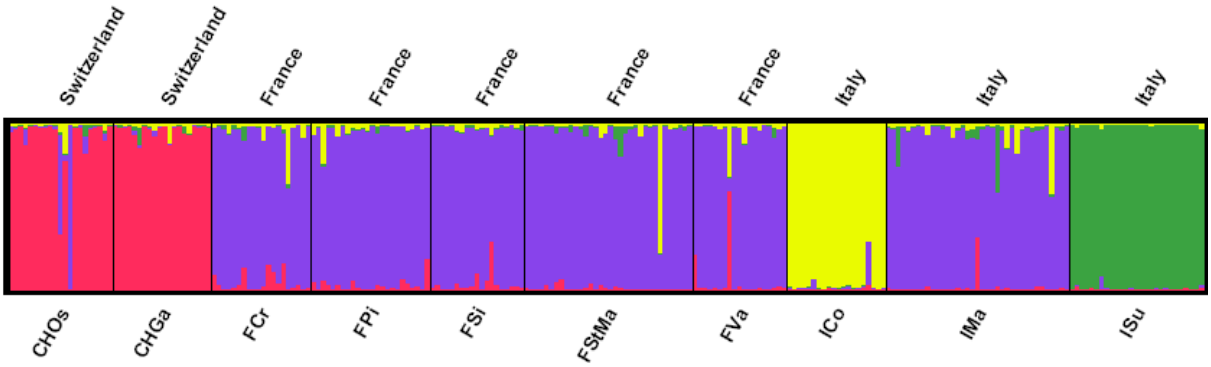

D (3x)

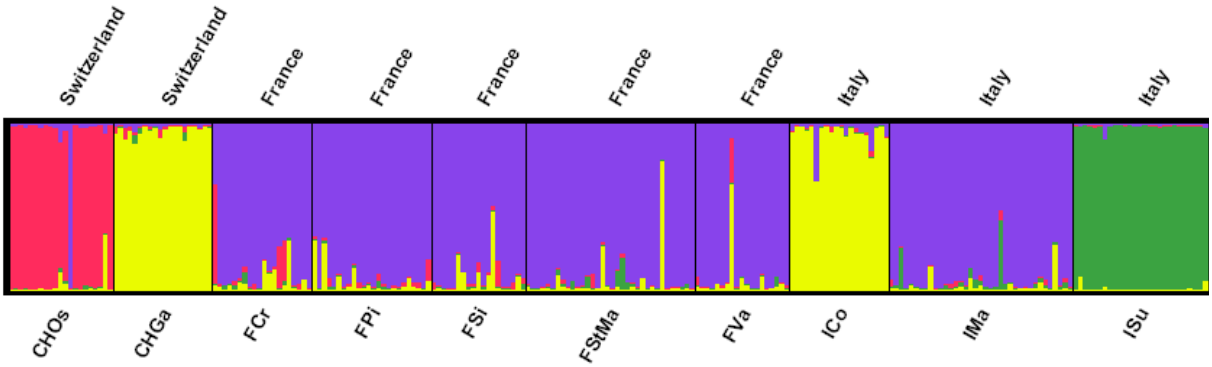

E (1x)

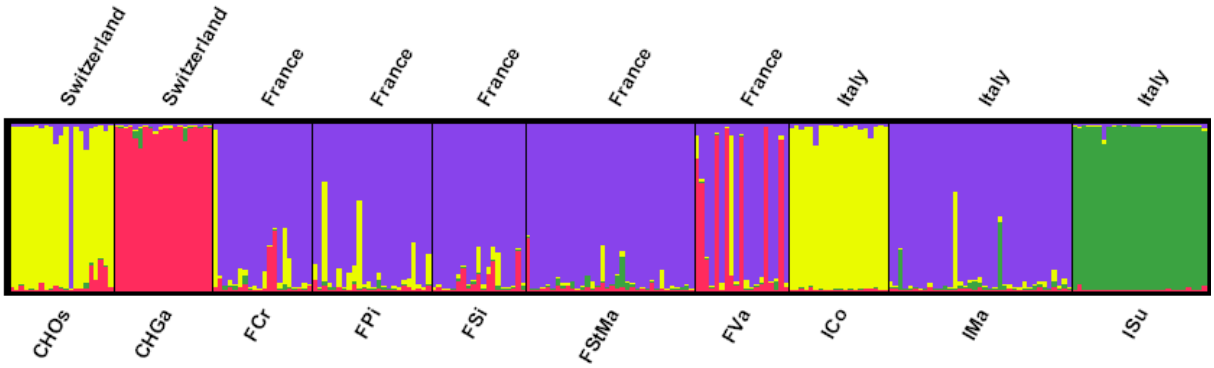

Appendix 15

The following Oedipodinae were used to reconstruct phylogenetic relationships based on 1040bp of the mitochondrial gene *ND2*. In addition, five samples of *Oedaleus decorus* collected in this study were included.

Species	GenBank Accession no
Aiolopus tamulus	EF395804.1
Angaracris barabensis	EF395798.1
Angaracris rhodops	EF395795.1
Bryodema luctuosum luctuosum	EF395800.1
Bryodema nigroptera	EF395802.1
Bryodema miramae miramae	EF395799.1
Bryodemella holdereri holdereri	EF395801.1
Compsorhipis davidiana	EF395737.1
Gastrimargus marmoratus	EF395793.1
Oedaleus decorus decorus	EF395792.1
Oedaleus infernalis	EF395790.1
Oedaleus manjius	EF395794.1
Sphingonotus tahulingensis	EF395794.1
Sphingonotus yanchihensis	EF395795.1
Trilophidia annulata	EF395803.1

Appendix 15A

Bayesian reconstruction of phylogenetic relationships based on 1040bp mtDNA (*ND2*) from 22 already published sequences of other Oedipodinae and five sequences of *Oedaleus decorus* collected in this study. Posterior probabilities are indicated and the phylogenetic tree was rooted with the outgroup *Acheta domesticus.*

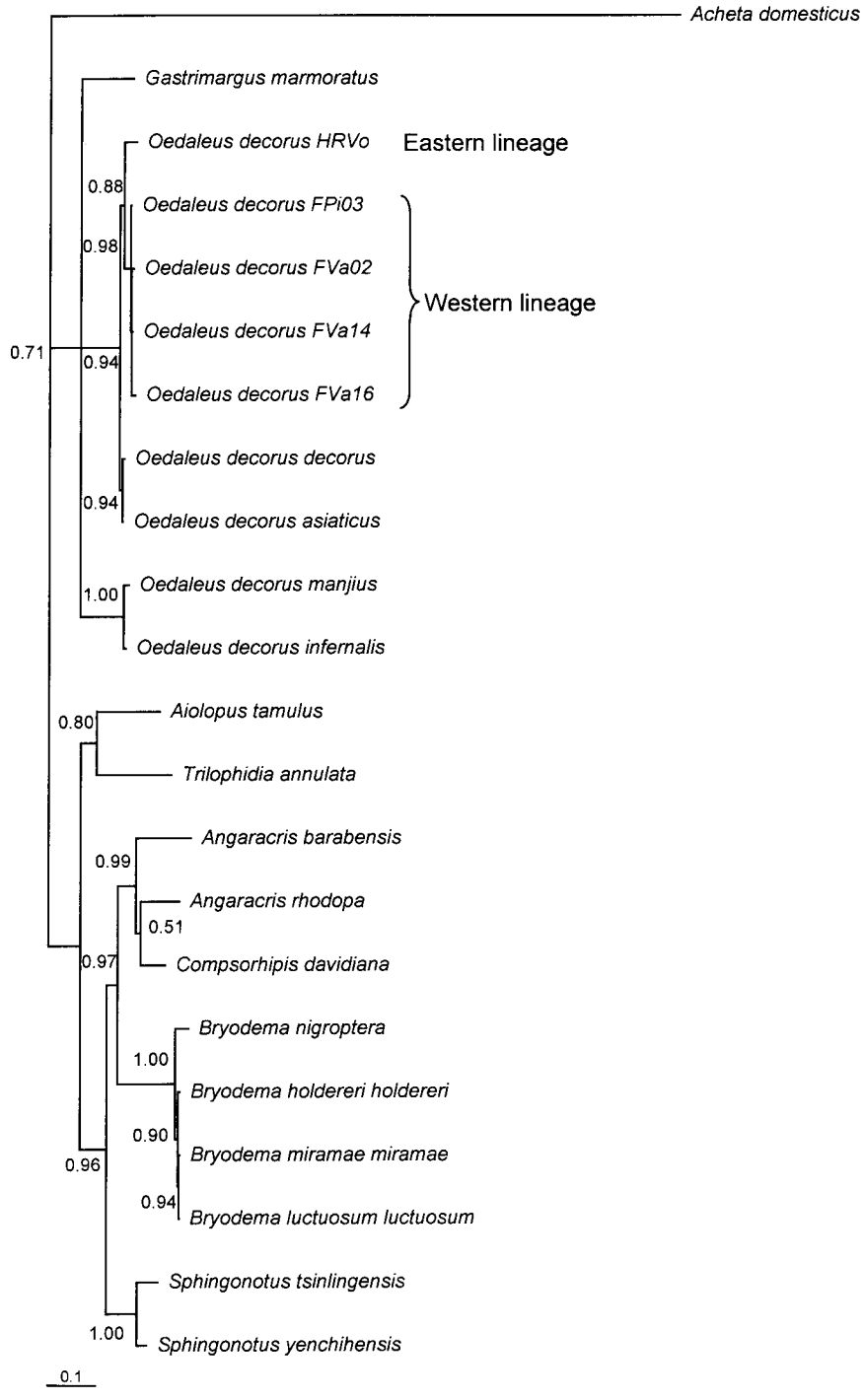

Appendix 15B

Phylogenetic relationships inferred with neighbour-joining algorithm based on 1040bp mtDNA (*ND2*) from 22 already published sequences of other Oedipodinae and five sequences of *Oedaleus decorus* collected in this study. Support values are indicated and the phylogenetic tree was rooted with the outgroup *Acheta domesticus.*